0026-895X/98/030573-17$3.00/0

MOLECULAR PHARMACOLOGY, **53:**573–589 (1998).

Subtype-Selective Positive Cooperative Interactions between Brucine Analogues and Acetylcholine at Muscarinic Receptors: Radioligand Binding Studies

S. LAZARENO, P. GHARAGOZLOO, D. KUONEN, A. POPHAM, and N. J. M. BIRDSALL

MRC Collaborative Centre (S.L., P.G., D.K., A.P.), Mill Hill, London NW7 1AD, UK, and the Division of Physical Biochemistry (N.J.M.B.), National Institute for Medical Research, Mill Hill, London NW7 1AA, UK

Received September 3, 1997; Accepted December 9, 1997

This paper is available online at http://www.molpharm.org

ABSTRACT

We studied the interactions of strychnine, brucine, and three of the *N*-substituted analogues of brucine with [^{3}H]*N*-methylscopolamine (NMS) and unlabeled acetylcholine at m1–m5 muscarinic receptors using equilibrium and nonequilibrium radioligand binding studies. The results were consistent with a ternary allosteric model in which both the primary and allosteric ligands bind simultaneously to the receptor and modify the affinities of each other. The compounds had K_d values in the submillimolar range, inhibited [^{3}H]NMS dissociation, and showed various patterns of positive, neutral, and negative cooperativity with [^{3}H]NMS and acetylcholine, but there was no predictive relationship between the effects. Acetylcholine affinity was increased ~2-fold by brucine at m1 receptors, ~3-fold by *N*-chloromethyl brucine at m3 receptors, and ~1.5-fold by brucine-*N*-oxide at m4 receptors. The existence of neutral cooperativity, in which the compound bound to the receptor but did not modify the affinity of acetylcholine, provides the opportunity for a novel form of drug selectivity that we refer to as absolute subtype selectivity: an agent showing positive or negative cooperativity with the endogenous ligand at one receptor subtype and neutral cooperativity at the other subtypes would exert functional effects at only the one subtype, regardless of the concentration of agent or its affinities for the subtypes. Our results demonstrate the potential for developing allosteric enhancers of acetylcholine affinity at individual subtypes of muscarinic receptor and suggest that minor modification of a compound showing positive, neutral, or low negative cooperativity with acetylcholine may yield compounds with various patterns of cooperativity across the receptor subtypes.

Muscarinic acetylcholine receptors couple to G proteins and are distributed widely throughout the periphery and central nervous system (Caulfield, 1993). The existence of five receptor subtypes, and their differential distribution in the central nervous system, offers scope for selective agonists and antagonists as therapeutic agents; possible therapeutic targets are Alzheimer's disease, Parkinson's disease, and schizophrenia (Ehlert *et al*., 1994; Yeomans, 1995). Currently available muscarinic drugs, however, show only modest subtype selectivity, perhaps because of the strong conservation of sequence in regions considered to bind agonists (Hulme *et al*., 1990).

Muscarinic receptors contain primary sites at which agonists and competitive antagonists bind and one or more allosteric sites that mediate the effects of various agents on the binding of ligands at the primary site (Tucek and Proska, 1995; Birdsall *et al*., 1996; Tränkle and Mohr, 1997). Gallamine, a widely used neuromuscular blocking agent, also is the prototypical muscarinic allosteric antagonist, and it seems to act at a common site with other allosteric antagonists, such as obidoxime, tubocurarine, and methoctramine (Ellis and Seidenberg, 1992; Waelbroeck, 1994). Antagonists acting wholly or in part through an allosteric mechanism are among the most subtype-selective muscarinic antagonists, perhaps because the allosteric site is in a less well conserved region of muscarinic receptors (Matsui *et al*., 1995; Tucek and Proska, 1995; Birdsall *et al*., 1996).

Allosteric action at muscarinic receptors usually is detected through the effect of an agent to inhibit the dissociation of radioligands, and compounds with such effects have almost always been found to act as inhibitors in equilibrium binding or functional studies (Tucek and Proska, 1995). The report of Tucek *et al*. (1990) provided the first clear demonstration that allosteric agents could exert positively cooperative effects at muscarinic receptors and provided a striking example of the importance of the receptor subtype and nature of the primary ligand on the direction of the cooperative interaction. These authors found that alcuronium, another

This work was funded by Sankyo Co. Ltd. (Tokyo, Japan) and the Medical Research Council (UK).

A brief description of some of the results has been reported previously (Birdsall *et al*., 1997).

ABBREVIATIONS: NMS, *N*-methylscopolamine; ACh, acetylcholine; CMB, *N*-chloromethyl brucine; BNO, brucine-*N*-oxide; HEPES, 4-(2-hydroxyethyl)-1-piperazineethanesulfonic acid; GABA, γ-aminobutyric acid.

An erratum has been published:
http://molpharm.aspetjournals.org/content/55/1/194.full.pdf

neuromuscular blocking agent, increased the affinity of the antagonist radioligand [^{3}H]NMS at M_2 receptors but reduced it at M_3 receptors; moreover, although alcuronium increased the binding of [^{3}H]NMS at M_2 receptors, it inhibited the binding of another antagonist radioligand, [^{3}H]QNB, at the same receptor subtype. There is no obvious physicochemical characteristic of the different antagonist radioligands to account for their differing cooperative effects with alcuronium (Hejnova *et al.*, 1995).

The observation that alcuronium increased the affinity of [^{3}H]NMS at m2 receptors implied that it might be possible to develop agents that could enhance the affinity of the endogenous neurotransmitter ACh at the m1 receptor. Strychnine, a glycine receptor antagonist and starting material in the synthesis of alcuronium, also increases the affinity of [^{3}H]NMS at m2 receptors (Lazareno and Birdsall, 1995; Proska and Tucek, 1995) and has only ~2-fold negative cooperativity with ACh at m1 receptors (Lazareno and Birdsall, 1995). *N*-Substituted analogues of strychnine show various patterns of positive and negative cooperativity with [^{3}H]NMS, but none increased the affinity of ACh (P. Gharagozloo, S. Lazareno, A. Popham, and N. J. M. Birdsall, in preparation).

One of our research aims has been to find compounds that are positively cooperative with ACh at one or more muscarinic receptor subtypes. We describe here the characterization of the allosteric binding properties of brucine (10,11-dimethoxy strychnine; Fig. 1) and three *N*-substituted analogues at the human muscarinic receptor subtypes. All compounds showed neutral or positive cooperativity with ACh at one or more receptor subtype. ACh affinity was increased 3-fold at m3 receptors by CMB, 2-fold at m1 receptors by brucine, and 1.4-fold at m4 receptors by BNO.

Experimental Procedures

Materials. [^{3}H]NMS (84–86 Ci/mmol) was from Amersham International. [^{3}H]ACh (75–85 Ci/mmol) was from Amersham International and ARC (St. Louis, MO). Strychnine HCl, brucine sulfate, and ACh chloride were from Sigma Chemical (Poole, Dorset, UK). BNO hydrate was from Aldrich Chemical (Poole, Dorset, UK). The preparation of the other *N*-substituted brucine analogues will be described elsewhere (P. Gharagozloo, S. Lazareno, A. Popham, and N. J. M. Birdsall, in preparation).

Cell culture and membrane preparation. Chinese hamster ovary cells stably expressing cDNA encoding human muscarinic m1–m5 receptors were generously provided by Dr. N. J. Buckley (University College London, London, UK). The cells were grown in α-minimum essential medium (GIBCO, Paisley, Scotland) containing 10% (v/v) newborn calf serum, 50 units/ml penicillin, 50 μg/ml streptomycin, and 2 mM glutamine at 37° under 5% CO_2. Cells were grown to confluence and harvested by scraping in a hypotonic medium (20 mM HEPES plus 10 mM EDTA, pH 7.4). Membranes were prepared at 0° by homogenization with a Polytron homogenizer (Brinkmann Instruments, Westbury, NY) followed by centrifugation (40,000 × *g*, 15 min), washed once in 20 mM HEPES plus 0.1 mM EDTA, pH 7.4, and stored at −70° in the same buffer at protein concentrations of 2–5 mg/ml. Protein concentrations were measured with the BioRad (Hemel Hempstead, UK) reagent using bovine serum albumin as the standard. The yields of receptor varied among batches but were ~5, ~1, ~7, ~2, and ~1 pmol/mg of total membrane protein for the m1, m2, m3, m4, and m5 subtype, respectively.

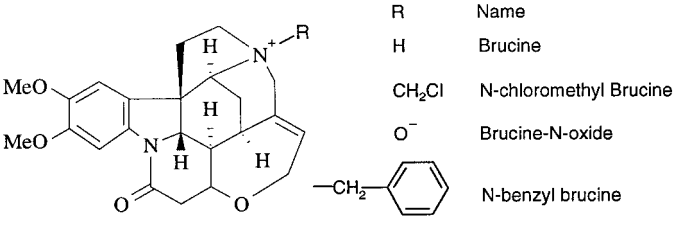

Fig. 1. Structure of brucine and its analogues.

Radioligand binding assays. Unless otherwise stated, frozen membranes were thawed; resuspended in a buffer containing 20 mM HEPES, 100 mM NaCl, and 10 mM $MgCl_2$, pH 7.4; and incubated with radioligand and unlabeled drugs for 2 hr at 30° in a volume of 1 ml. Membranes were collected by filtration over glass-fiber GF/B filters (Whatman, Maidstone, UK) presoaked in 0.1% polyethylenimine with a Brandel cell harvester (Semat, Herts, UK), extracted overnight in scintillation fluid (ReadySafe; Beckman, Columbia, MD), and counted for radioactivity in Beckman LS6000 scintillation counters. Membrane protein concentrations (5–50 μg/ml) were adjusted so no more than ~15% of added radioligand was bound. Nonspecific binding was measured in the presence of 10^{-6} M QNB (an antagonist with picomolar potency) and accounted for 1–5% of total binding. GTP was present at a concentration of 2×10^{-4} M in assays containing unlabeled ACh. Binding of [^{3}H]ACh (5–10 nM) to m2 and m4 receptors was measured in a volume of 250 μl after a 1-hr incubation. Data points usually were measured in duplicate. Chinese hamster ovary cell membranes do not possess cholinesterase activity (Lazareno and Birdsall, 1993; Gnagey and Ellis, 1996), so ACh could be used in the absence of a cholinesterase inhibitor. Most brucine analogues were dissolved in dimethylsulfoxide, which at the highest final concentration of 1%, had no effect on binding. CMB was dissolved in water, and BNO was dissolved in buffer.

Experimental design and data analysis. The four types of assay used in this study are described below, and the equations shown are based on equations derived previously (Lazareno and Birdsall, 1995). General data preprocessing, as well as the affinity ratio calculations and routine plots of the semiquantitative equilibrium assay, were performed using Minitab (Minitab Ltd., Coventry, UK). The other three assays were analyzed with nonlinear regression analysis using the fitting procedure in SigmaPlot (SPSS, Erkrath, Germany). This procedure is relatively powerful in that it allows the use of two or more independent variables (e.g., concentrations of two drugs); this is required for the analysis of the quantitative equilibrium and nonequilibrium assays. Unless otherwise stated, data are presented as mean ± standard error.

Semiquantitative equilibrium assay to estimate cooperativity between an agent and both [^{3}H]NMS and unlabeled ACh and affinity of the agent for the receptor. Binding data were obtained with a low concentration of [^{3}H]NMS (0.2 nM for m1, m3, and m4 receptors; 0.4 nM for m2 receptor; 0.7 nM for m5 receptor) in the absence and presence of a number of concentrations of the agent (typically three) in the absence and presence of a fixed concentration of ACh (20 μM for m1 and m3 receptors; 2 μM for m2 receptor; 5 μM for m4 receptor; 13 μM for m5 receptor). The binding of a high concentration of [^{3}H]NMS alone (2–5 nM) also was measured. The data were transformed into affinity ratios [ratios of apparent affinity of the ligand ([^{3}H]NMS or ACh) in the presence of the agent compared with the affinity of ligand alone (Lazareno and Birdsall, 1995)].

The calculations are as follows. Specific binding was obtained by subtracting nonspecific from total binding. Free radioligand (dpm) was obtained by subtracting total binding with [^{3}H]NMS alone from that with added dpm.

The B_{max} value was calculated with the equation

$$B_{max} = \frac{B_{L_1} \cdot B_L \cdot (L - L_1)}{L \cdot B_{L_1} - L_1 \cdot B_L} \quad (1)$$

where L_1 and L are the high and low free concentrations of [^{3}H]NMS, respectively, and B_{L_1} and B_L are the corresponding levels of specific binding in the absence of additional ligands, respectively.

The apparent affinity constant, K_{LX}, of [^{3}H]NMS in the presence of a particular concentration of test agent was estimated with the equation

$$K_{LX} = \frac{B_{LX}}{L \cdot (B_{max} - B_{LX})} \quad (2)$$

where B_{LX} is specific binding in the presence of test agent alone.

The apparent affinity constant, K_{AX}, of ACh in the presence of the test agent alone was estimated with the equation

$$K_{AX} = \frac{B_{max}(B_{LX} - B_{LAX})}{A \cdot B_{LAX}(B_{max} - B_{LX})} \quad (3)$$

where A is the fixed concentration of ACh, and B_{LAX} is specific binding in the presence of both ACh and test agent.

These apparent affinities, K_{LX} and K_{AX}, were divided by the "true" affinities (measured in the absence of test agent) to obtain the affinity ratios of [^{3}H]NMS and ACh. Values of affinity ratio of >1 suggest the presence of positive cooperativity. Values of affinity ratio of <1 for which the asymptotic value, at high concentrations of agent, is >0 suggest weak negative cooperativity, whereas values of affinity ratio of <1, which tend to an asymptote of 0, suggest strong negative cooperativity or a competitive interaction. This affinity ratio measure is in principle independent of the fixed concentrations of [^{3}H]NMS and ACh, and the fractional effect of the test agent on the affinity ratio, relative to its maximal effect, corresponds to the fractional occupancy of the agent for the receptor in the absence of other ligands (Lazareno and Birdsall, 1995).

The assay was conducted in the presence of 2×10^{-4} M GTP to minimize high affinity ACh binding. Nevertheless, the Hill slopes of ACh inhibition curves under these conditions were <1 (~0.8–1) at all subtypes, which violates one of the assumptions of the analysis (that the Hill slope of ACh binding is 1). Although this violation may introduce a small quantitative error into the estimates of ACh affinity, the value of the affinity ratio of ACh can be shown to be independent of the slope of ACh binding (see Appendix).

Off-rate assay to estimate affinity of an allosteric agent for the [^{3}H]NMS-occupied receptor. A high concentration of membranes (2–4 mg of protein/ml) was incubated with a high concentration of [^{3}H]NMS (5 nM) for ~15 min. Then, 10-μl aliquots were distributed into tubes that were empty or contained 1 ml of 10^{-6} M QNB alone and in the presence of a number of concentrations of allosteric agent (typically four). Nonspecific binding was measured in separately prepared tubes containing 10 μl of membrane and 2 μl of [^{3}H]NMS plus QNB. Later (~2.5 dissociation half-lives; see Table 2), the samples were filtered. The data were transformed to rate constant k_{off} using the formula $k_{off} = \ln(B_0/B_t)/t$, where B_0 is initially bound radioligand, and B_t is bound radioligand remaining after time t (min of dissociation). These values were expressed as percentage of inhibition of the true [^{3}H]NMS dissociation rate constant (k_{off} in the absence of allosteric agent) and fitted to a hyperbolic function using nonlinear regression analysis. The curves were well fitted with slopes fixed at 1; the observed maximum inhibition was not consistently different from 100% and was usually fixed to 100%, but these points were not investigated explicitly. As with strychnine at m1–m4 receptors (Lazareno and Birdsall, 1995), the dissociation of [^{3}H]NMS from m2 receptors in the absence and presence of various concentrations of brucine was monophasic and consistent with the allosteric model (data not shown). With the assumption of a similar behavior by brucine and its analogues at all the muscarinic receptors, the inhibition curves correspond theoretically to the occupancy curves of the allosteric agents at the [^{3}H]NMS-occupied receptors, regardless of whether the inhibition of [^{3}H]NMS dissociation is caused by an allosteric change in the shape of the receptor or the trapping of the [^{3}H]NMS in its binding pocket by the bound allosteric agent (Lazareno and Birdsall, 1995).

Equilibrium assay for quantitative estimation of affinity of an allosteric agent for the receptor and magnitude of its cooperativity with [^{3}H]NMS and ACh. The binding of [^{3}H]NMS (0.2 nM for m1, m3, and m4 receptors; 0.4 nM for m2 receptors; 0.7 nM for m5 receptors) was measured alone and in the presence of six concentrations of ACh, alone and in the presence of three concentrations of test agent. Binding with a high concentration of [^{3}H]NMS also was measured, allowing the B_{max} value to be estimated using eq. 1. The specific binding data were subjected to nonlinear regression analysis using the equation

$$B_{LAX} = \frac{B_{max} \cdot L \cdot K_L(1 + \alpha \cdot X \cdot K_X)}{1 + X \cdot K_X + (A \cdot K_A)^n \cdot (1 + \beta \cdot X \cdot K_X) + L \cdot K_L(1 + \alpha \cdot X \cdot K_X)} \quad (4)$$

where B_{LAX} is the observed specific bound radioligand; B_{max} was calculated with eq. 1; L, A, and X are concentrations of [^{3}H]NMS, ACh, and allosteric agent, respectively; K_L, K_A, and K_X are affinity constants for the corresponding ligands and the receptor; α and β are allosteric constants of X with [^{3}H]NMS and ACh, respectively; and n is a logistic slope factor to describe the binding of ACh. K_d values for [^{3}H]NMS from these assays were 111 ± 12 (13 determinations), 337 ± 34 (12 determinations), 211 ± 16 (12 determinations), 78 ± 7 (12 determinations), and 603 ± 35 (6 determinations) pM, corresponding to log affinity values of 9.95, 9.47, 9.68, 10.11, and 9.22 M^{-1} at m1–m5 receptors, respectively.

Above a certain concentration, some allosteric agents, especially those that exhibit neutral or positive cooperativity with [^{3}H]NMS, may slow the kinetics of [^{3}H]NMS binding so much that the binding does not reach equilibrium. In most cases, sufficient incubation time was used to allow [^{3}H]NMS binding in the presence of the agent to reach equilibrium. In a few cases, however, the highest concentration of agent would be predicted to slow [^{3}H]NMS kinetics sufficiently to prevent binding equilibrium from being reached, and in these cases the data were better fitted to the equation

$$B_{LAXt} = B_{LAX} + \left[(B_{L_0} - B_{LAX}) \cdot \left(\exp\left(\frac{-t \cdot k_{off}}{1 - \alpha \cdot X \cdot K_X} + \frac{-t \cdot k_{off} \cdot L \cdot K_L}{1 + X \cdot K_X + (A \cdot K_A)^n \cdot (1 + \beta \cdot X \cdot K_X)} \right) \right) \right] \quad (5)$$

where B_{LAXt} is observed specific binding under nonequilibrium conditions, B_{LAX} is the predicted equilibrium binding defined in eq. 4, t is the incubation time, k_{off} is the dissociation rate constant of [^{3}H]NMS, and B_{L_0} is the initial amount of bound radioligand, set to zero in this case. This equation assumes that the dissociation of [^{3}H]NMS from the allosteric agent-occupied receptor is negligible and that the binding kinetics of both ACh and the allosteric agent are fast in comparison with the dissociation rate of [^{3}H]NMS.

Nonequilibrium assay to estimate the affinity of an allosteric agent for the receptor and its cooperativity with [^{3}H]NMS. Solutions/suspensions of [^{3}H]NMS and membranes were prepared at 100 times their final concentration. Prelabeling of receptors was achieved by mixing equal portions of the [^{3}H]NMS solution and membrane suspension; the concentration of [^{3}H]NMS in the mixture was 50 times greater than its final concentration, so almost the entire receptor population would be labeled within 1–2 min. Tubes were prepared containing 1 ml of allosteric agent at its final concentration.

The incubation was initiated by adding unlabeled membranes or the equilibrated membrane/ [^{3}H]NMS mixture to the appropriate set of tubes. There were two sets of tubes. Set A tubes received 20 μl of the membrane/[^{3}H]NMS mixture, which had been prepared ≥5 min earlier. Set B tubes received 10 μl of [^{3}H]NMS followed by 10 μl of membranes. The incubation proceeded at 30° for ~10 [^{3}H]NMS dissociation half-lives (see Table 2 and legend to Fig. 4). After dilution

in allosteric agent, set A tubes attain equilibrium through dissociation of [^{3}H]NMS. Kinetic-slowing effects in set A tubes are seen as an increase in binding above the equilibrium level, whereas the equivalent effect in set B tubes is seen as decreased binding. The data for both sets of tubes were analyzed simultaneously through nonlinear regression by fitting the specific binding data to eq. 5 with A set to zero. B_{L_0} is the initial level of binding: for prelabeled membranes of set A tubes in the presence of 50 times the final radioligand concentration, L, the initial binding is given by

$$B_{L_o} = \frac{B_{max} \cdot 50 \cdot L \cdot K_L}{1 + 50 \cdot L \cdot K_L} \quad (6)$$

and for the initially unlabeled membranes of set B tubes, $B_{L_0} = 0$.

In some cases, in the presence of zero and low concentrations of allosteric agent, binding was slightly different (<5%) between the two sets of tubes. This was assumed to reflect differences in the B_{max} values, and probably the quantity of membranes, in the two sets of tubes. In such cases, the data of the set B tubes were scaled using data obtained with inactive concentrations of allosteric agent.

The precision with which the parameters are defined by the data depends on the size of the allosteric effect of the test agent; if the agent has neutral or low cooperativity with [^{3}H]NMS, then only the kinetic effects are clearly seen. The dissociation rate constants of [^{3}H]NMS always were fixed to known values (0.07, 0.35, 0.08, and 0.06 min^{-1} at m1–m4 receptors, respectively), and in some cases the K_d value of [^{3}H]NMS also was fixed. All other parameters (B_{max}, α, and K_X) were estimated.

Results

Allosteric agents affect both the equilibrium binding of labeled and unlabeled muscarinic ligands and the dissociation of bound radioligand, and the two effects can be related using a ternary allosteric model (Lazareno and Birdsall, 1995). We initially assessed compounds with a semiquantitative equilibrium assay (Fig. 2) and a single-time point off-rate assay (Fig. 3).

Fig. 2A shows specific [^{3}H]NMS binding at m2 and m3 receptors in the presence of three concentrations of *N*-benzyl brucine, alone and in the presence of a single concentration of ACh. The binding of [^{3}H]ACh at m2 receptors also is shown. It is obvious from Fig. 2A that *N*-benzyl brucine increased [^{3}H]NMS binding at m2 receptors, decreased [^{3}H]NMS binding at m3 receptors, and decreased [^{3}H]ACh binding at m2 receptors. *N*-Benzyl brucine had similar effects on [^{3}H]NMS binding in the absence and presence of unlabeled ACh (i.e., an increase at m2 receptors and a decrease at m3 receptors), but the effects of *N*-benzyl brucine on the binding of unlabeled ACh itself are not clear based on the plots of raw data shown in Fig. 2A. When the data are transformed to affinity ratios (Fig. 2B), however, it becomes apparent that *N*-benzyl brucine decreased the binding of unlabeled ACh at m2 receptors over a similar concentration range and to a similar extent with which it inhibited [^{3}H]ACh binding at m2 receptors; at m3 receptors, in contrast, *N*-benzyl brucine increased the binding of unlabeled ACh. Semiquantitative estimates of the cooperativity of *N*-benzyl brucine are presented in Table 1, together with data for other brucine analogues (see below).

In addition to its effects on the equilibrium binding of [^{3}H]NMS, *N*-benzyl brucine acted at [^{3}H]NMS-occupied receptors to inhibit the dissociation rate of [^{3}H]NMS (Fig. 3). *N*-Benzyl brucine was most potent at the [^{3}H]NMS-occupied m2 receptor, with an IC_{50} value of ~10 μM; ~3-fold weaker at [^{3}H]NMS-occupied m1 and m4 receptors; and ~20-fold weaker at [^{3}H]NMS-occupied m3 and m5 receptors.

Table 2 shows affinity estimates at [^{3}H]NMS-occupied m1–m5 receptors for brucine and three analogues obtained with the off-rate assay. Data also are shown for strychnine. In general, the compounds did not discriminate among m1, m2, and m4 receptors but were ~10-fold weaker at m3 receptors and even weaker at m5 receptors. Brucine was ~3-fold less potent than strychnine, except at m3 receptors, where it was 10-fold less potent. The *N*-chloromethyl and *N*-benzyl analogues of brucine had similar affinities to the parent, whereas brucine-*N*-oxide was ~10-fold less potent.

Three compounds that revealed different patterns of positive cooperativity with ACh in the semiquantitative equilibrium assay were selected for more detailed study, both to confirm and quantify the allosteric effects and to assess quantitatively whether the equilibrium and kinetic effects of the compounds were mutually consistent with the ternary allosteric model. Brucine, CMB, and BNO were studied using two types of assay: a nonequilibrium and an equilibrium assay. The parameter estimates for these compounds and for strychnine from both types of assay are summarized in Tables 3-6.

The nonequilibrium assay is based on the fact that the effect of these agents to slow [^{3}H]NMS dissociation (Fig. 3) also results in slowing of [^{3}H]NMS association, to the extent that at high concentrations of agent, [^{3}H]NMS binding will not reach equilibrium. In such a case, the inhibition of [^{3}H]NMS binding reflects a nonequilibrium kinetic artifact, but it may be mistaken for negative cooperativity. The nonequilibrium assay simultaneously measures both equilibrium and nonequilibrium effects on [^{3}H]NMS binding by starting the assay with both [^{3}H]NMS-prelabeled and empty receptors. The data are used to estimate the affinity of the agent and its cooperativity with [^{3}H]NMS (see Experimental Procedures). Fig. 4 shows data from such an assay with CMB at m1–m4 receptors. It is clear that at high concentrations of CMB (≥0.3 mM for at m1, m2, and m4 receptors; ≥1 mM for at m3 receptors), the inhibition of [^{3}H]NMS binding to nonprelabeled receptors reflects a failure of the binding to reach equilibrium. In contrast, the reduction of [^{3}H]NMS binding to both prelabeled and nonprelabeled m3 receptors by lower concentrations of CMB reflects a negatively cooperative interaction with [^{3}H]NMS.

The quantitative equilibrium assay measures inhibition of [^{3}H]NMS binding by ACh (in the presence of GTP) in the presence of various concentrations of the agent, allowing estimates to be made of the affinity of the agent and its cooperativity with both [^{3}H]NMS and ACh (see Experimental Procedures). Data for the three brucine analogues are shown in Figs. 5-7. The patterns of cooperative interactions with [^{3}H]NMS and ACh are more clearly visualized by affinity ratio plots [the affinity ratio is 1/dose ratio (i.e., the ratio of apparent affinities of [^{3}H]NMS and ACh in the presence and absence of the allosteric agent)]. Figs. 5-7 (*insets*) show affinity ratios derived from the fitted values of the model parameters.

Tables 3–6 show that for each compound, the two types of assay yielded similar estimates of the affinity of the agent for the free receptor and its cooperativity with [^{3}H]NMS; the 12 values of the difference between the mean log affinity estimates for the free receptor from the two types of assay in

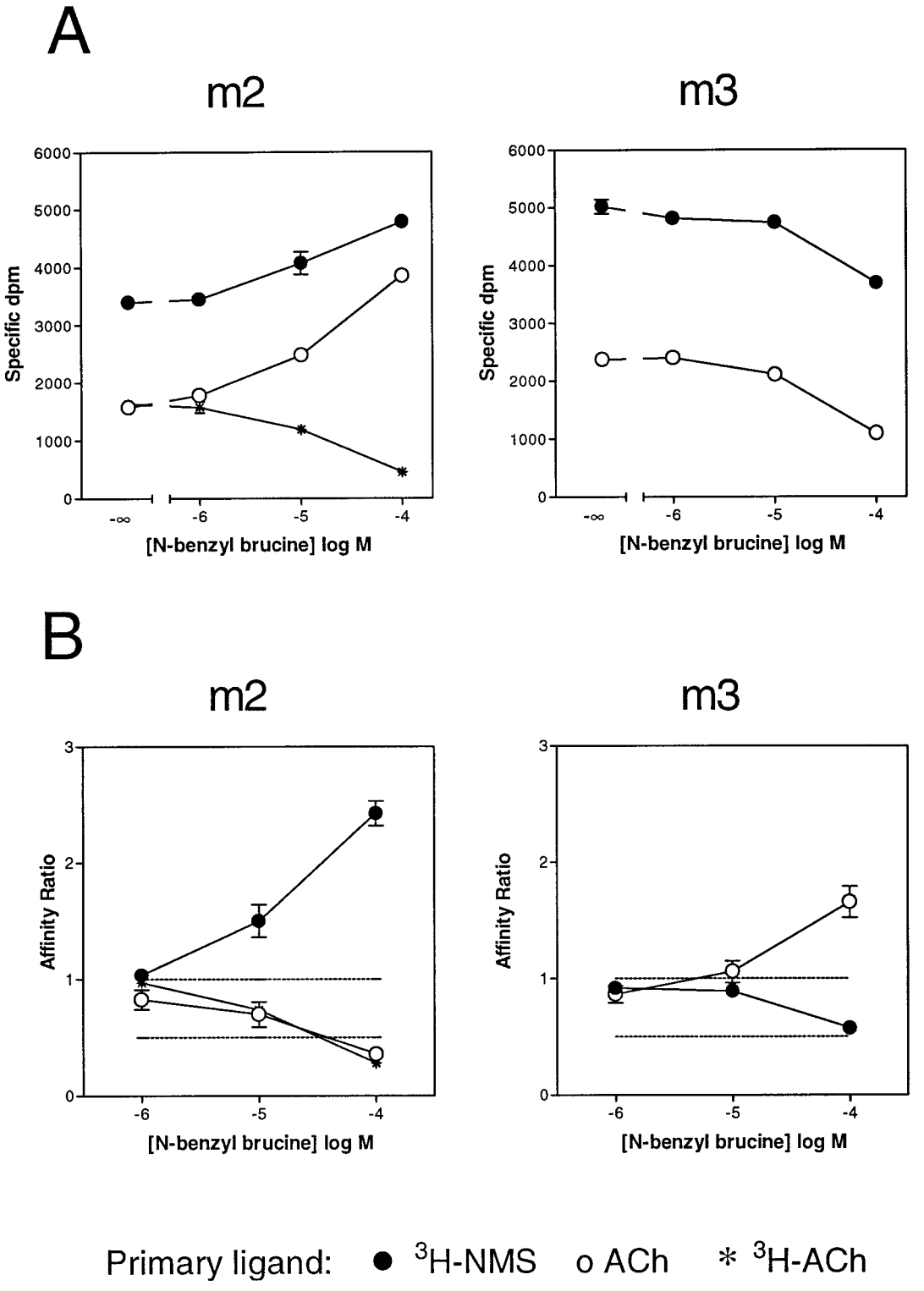

Fig. 2. Semiquantitative equilibrium assay with *N*-benzyl brucine at m2 and m3 receptors. A, Effects of *N*-benzyl brucine on [^{3}H]NMS binding in the absence and presence of unlabeled ACh (2 μM at m2 receptors, 20 μM at m3 receptors) in the presence of 0.2 mM GTP and on [^{3}H]ACh binding to m2 receptors measured in the absence of GTP. Data are the mean and range/2 of duplicate measures, except for the binding of [^{3}H]NMS alone, which was measured in quadruplicate. B, Affinity ratios calculated from the [^{3}H]NMS data in A. The fractional effect of *N*-benzyl brucine on the binding of [^{3}H]ACh at m2 receptors also is shown. The standard errors were calculated as described in the Appendix.

Tables 3–5 have a mean of 0.06 with a standard deviation of 0.18. The product of the affinity at the free receptor and cooperativity with [^{3}H]NMS provides an estimate of the affinity of the compound for the [^{3}H]NMS-occupied receptor, and these estimates from the two types of assay are in good agreement with each other and with the corresponding values measured directly in the off-rate assay (Table 2).

Table 1 shows a semiquantitative description of the coop-

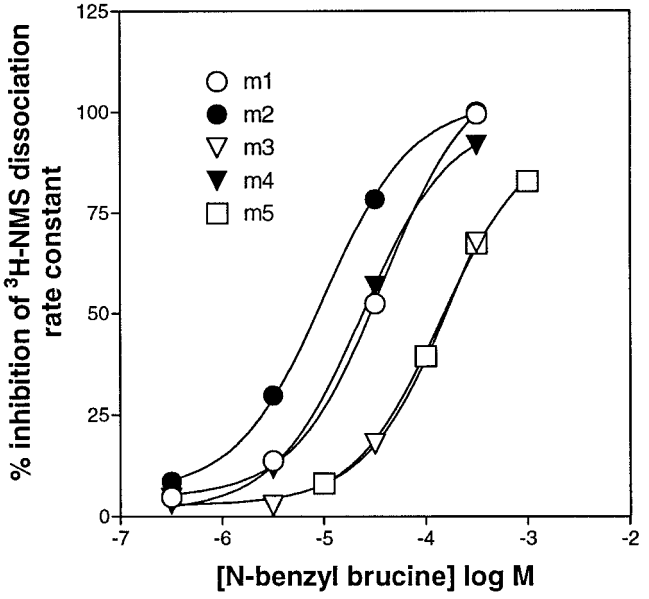

Fig. 3. Inhibition of [^{3}H]NMS dissociation from m1–m5 receptors by *N*-benzyl brucine. Prelabeled membranes were diluted into 1 μM QNB containing various concentrations of *N*-benzyl brucine, and after a fixed time (20 min for m1, 4 min for m2, 25 min for m3 and m4, and 44 min for m5), the samples were filtered. The data were transformed to rate constants (see Experimental Procedures) and are expressed as percentage inhibition of the control dissociation rate constant. The data are from a single experiment conducted in duplicate. *Lines*, fit of the data to a hyperbolic function.

TABLE 1

Estimates of cooperativity of brucine analogues with [^{3}H]NMS and ACh at muscarinic receptors

Values of cooperativity (shown as symbols) for brucine, CMB, BNO, and strychnine are from the results of detailed experiments summarized in Tables 3–6.

Values for *N*-benzyl brucine were derived from results with the semiquantitative equilibrium assay together with the results of the off-rate assay, each with at least two experiments. The logic for analyzing these results is described in the Appendix.

	m1	m2	m3	m4	m5
Cooperativity with [^{3}H]NMS					
Brucine	0	+	–	–	– –
CMB	–	+	–	0	–
BNO	+	++	0	0	+
N-Benzyl brucine	–	++	–	0	0
Strychnine	0	++	–	+	– –
Cooperativity with ACh					
Brucine	+	–	–	–	– –
CMB	–	– –	++	0	– –
BNO	0	–	++	+	–
N-Benzyl brucine	–	–	+	–	–
Strychnine	–	– –	– –	–	– –

– –, <0.2; –, 0.2–0.8; 0, 0.81–1.19; +, 1.2–2; ++, >2.

erativity of four brucine analogues and strychnine with [^{3}H]NMS and ACh. The m1, m3, and m4 subtypes supported positive cooperativity between ACh and at least one of the compounds.

With regard to [^{3}H]NMS binding, the degree of cooperativity across receptor subtypes showed the pattern m2 > m4 ≥ 1 ≥ m1 ≥ m3 ≥ m5. All the compounds increased [^{3}H]NMS binding at m2 receptors; BNO had small positive effects at m1 and m5 receptors; and strychnine had a small positive effect at m4 receptors. All compounds showed neutral cooperativity with [^{3}H]NMS at one or more subtypes (i.e., the agent bound to the receptor and affected [^{3}H]NMS dissociation rate, and in some instances the affinity of ACh, but did not alter the affinity of [^{3}H]NMS). All compounds except BNO showed negative cooperativity with [^{3}H]NMS at one or more subtypes.

With regard to ACh, the degree of cooperativity across subtypes showed the general pattern m3 > 1 > m4 ≥ m1 > m2 = m5. ACh affinity was enhanced ~2-fold by brucine at m1 receptors, ~1.5-fold by BNO at m4 receptors, and 3-fold by CMB and BNO (and to a lesser degree by *N*-benzyl brucine) at m3 receptors. There were two instances of neutral cooperativity: with BNO at m1 receptors and CMB at m4 receptors. All the compounds were negatively cooperative to some degree with ACh at m2 and m5 receptors. Strychnine was negatively cooperative with ACh at all subtypes. Brucine and *N*-benzyl brucine had positive cooperativity at one subtype and negative cooperativity at the remainder, but the subtype supporting positive cooperativity was m1 with brucine and m3 with *N*-benzyl brucine. These results indicate that brucine and some analogs show a wide range of patterns of negative, neutral, and positive cooperativity with ACh across the receptor subtypes. Each compound has a unique pattern of cooperativity, and there is no significant correlation between cooperativity with [^{3}H]NMS and ACh ($p > 0.05$, Spearman's rank correlation), indicating that for this series of compounds, the cooperativity with [^{3}H]NMS of a particular compound acting at a particular receptor is a poor predictor of its cooperativity with ACh.

The positive effect of brucine on [^{3}H]NMS binding at m2 receptors was studied further using a range of [^{3}H]NMS and brucine concentrations and was found to result from a concentration-dependent decrease in the K_d value of [^{3}H]NMS with no consistent change in the B_{max} value (Fig. 8). The parameter estimates from five such experiments, giving a K_d value for [^{3}H]NMS of 0.33 ± 0.02 nM, log affinity of brucine of 4.42 ± 0.01, and cooperativity of 1.49 ± 0.04, are entirely consistent with estimates of equivalent parameters obtained with a single [^{3}H]NMS concentration and shown in Table 3.

The semiquantitative equilibrium assay (Fig. 2) also contains measures of the direct binding of [^{3}H]ACh at m2 and m4 receptors in the absence of GTP. Under these conditions, [^{3}H]ACh binds mainly to the receptor/G protein complex, whereas unlabeled ACh in the presence of GTP binds mainly to the uncoupled receptor. [^{3}H]ACh binding was not increased by any compound at m2 receptors but was increased at m4 receptors by one compound, BNO (data not shown). In further experiments, this effect was found to be concentration dependent (Fig. 9), with BNO increasing [^{3}H]ACh binding by 97 ± 11% with a $-\log EC_{50}$ value of 3.7 ± 0.2 (three experiments), indicating that BNO has similar affinity and cooperativity with ACh at G protein-coupled and -uncoupled m4 receptors.

Discussion

Strychnine and brucine are alkaloids isolated from *Strychnos nux-vomica*, which bind to glycine receptors with K_d values of ~10 and ~140 nM, respectively (Mackerer *et al.*, 1977; Marvizon *et al.*, 1986). These alkaloids allosterically inhibit glycine binding (Marvizon *et al.*, 1986), which presumably accounts for their convulsive effects in mice (Mackerer *et al.*, 1977). Brucine also has been reported to have other effects that presumably are unrelated to glycine receptors (Squires and Saederup, 1987; Ebihara and Akaike, 1992; Farrington *et al.*, 1994). The results reported here demonstrate that brucine also acts at an allosteric site on the muscarinic m1 receptor, at which it binds with a K_d value of ~30 μM and increases the affinity of ACh by ~2-fold. The

TABLE 2

Estimates of [^{3}H]NMS log affinity (log M^{-1}) of brucine analogues at [^{3}H]NMS-occupied muscarinic receptors

Values are shown as mean ± standard error (n) and were derived from the single-time point off-rate assay data as described in the text.

The dissociation times were 20, 4, 25, 25, and 44 min for m1—m5 receptors, respectively.

The [^{3}H]NMS dissociation rate constants (min^{-1}) measured at these dissociation times were 0.075 ± 0.006, 0.361 ± 0.018, 0.064 ± 0.003, 0.066 ± 0.003, and 0.033 ± 0.001 for m1—m5 receptors, respectively, with n = 13 for m1—m4 receptors and n = 7 for m5 receptors, corresponding to dissociation half-lives of 9.2, 1.9, 10.8, 10.5, and 21 min, respectively.

Analogue	Receptor subtype				
	m1	m2	m3	m4	m5
Brucine	4.50 ± 0.06 (5)	4.62 ± 0.05 (3)	3.21 ± 0.15 (5)	4.52 ± 0.06 (5)	2.94 ± 0.08 (2)
CMB	4.09 ± 0.05 (5)	4.63 ± 0.03 (4)	3.27 ± 0.12 (6)	4.37 ± 0.08 (6)	3.20 ± 0.02 (2)
BNO	3.23 ± 0.06 (6)	3.49 ± 0.03 (4)	2.52 ± 0.04 (6)	3.55 ± 0.05 (6)	2.33 ± 0.03 (2)
N-Benzyl brucine	4.37 ± 0.05 (3)	4.84 ± 0.13 (3)	3.77 ± 0.05 (3)	4.53 ± 0.08 (3)	3.72 ± 0.01 (2)
Strychnine[a]	4.9	5.2	4.2	5.0	3.62 ± 0.05 (2)

[a] Values at m1—m4 receptors are from Lazareno and Birdsall (1995).

TABLE 3

Parameters for the interaction of brucine with [^{3}H]NMS and ACh at m1—m5 muscarinic receptors

Subtype	Assay	Log affinity		Cooperativity		n
		Unoccupied receptor	[^{3}H]NMS-occupied receptor	[^{3}H]NMS	ACh	
m1	Nonequilibrium	4.73 ± 0.02	4.68 ± 0.05	0.87 ± 0.08		3
	Equilibrium	4.58 ± 0.05	4.54 ± 0.07	0.91 ± 0.04	1.60 ± 0.10[a]	5
m2	Nonequilibrium	4.25 ± 0.06	4.53 ± 0.04	1.91 ± 0.04		3
	Equilibrium	4.53 ± 0.04	4.74 ± 0.05	1.59 ± 0.06	0.28 ± 0.05	4
m3	Nonequilibrium	3.70 ± 0.05	3.51 ± 0.04	0.52 ± 0.01		2
	Equilibrium	3.52 ± 0.08	2.92 ± 0.13	0.25 ± 0.03	0.52 ± 0.10	4
m4	Nonequilibrium	4.63 ± 0.05	4.54 ± 0.03	0.84 ± 0.09		4
	Equilibrium	4.77 ± 0.15	4.49 ± 0.13	0.54 ± 0.06	0.33 ± 0.11	4
m5	Nonequilibrium					
	Equilibrium	4.31 ± 0.06	3.29 ± 0.02	0.10 ± 0.02	0.07 ± 0.01	2

[a] Significantly different from 1, $p < 0.005$, two-tailed t test.

2–4-fold positive cooperativity observed here between brucine analogues and ACh at certain muscarinic receptors is similar in magnitude to the positive cooperativity between therapeutically effective benzodiazepine tranquilizers and GABA at $GABA_A$ receptors (Ehlert *et al*., 1983)

This is the first report of agents that enhance ACh affinity through a well defined allosteric interaction at the muscarinic receptor [while this manuscript was in review, Jakubik *et al*. (1997) reported studies of allosteric effects of brucine and other agents on the binding of ACh and other agonists at muscarinic m1–m4 receptors]. The binding of a different muscarinic agonist, [^{3}H]oxotremorine-M, was slightly enhanced by tubocurarine (Waelbroeck *et al*., 1988), an agent that binds allosterically to muscarinic receptors and has low negative cooperativity with [^{3}H]NMS (Waelbroeck, 1994); it has not been possible, however, to repeat this observation using different batches of tubocurarine (Lazareno S, unpublished observations; Waelbroeck M, personal communication). The binding affinity of muscarinic agonists also can be increased with divalent cations (reviewed in Birdsall and Hulme, 1989) and by the sodium channel activator batrachotoxin (Minton and Sokolovsky, 1990).

We studied the allosteric interactions of brucine and some of its *N*-substituted analogues with [^{3}H]NMS and unlabeled ACh at muscarinic receptors by using a novel and efficient semiquantitative equilibrium assay. This assay was sufficiently sensitive to allow us to detect the small (≤2-fold) degree of positive cooperativity between brucine and ACh at m1 receptors. Considered in conjunction with the results of an assay to measure effects of the agent on radioligand dissociation, the semiquantitative equilibrium assay can indicate both the affinity of a test agent and its allosteric effect on an unlabeled compound (e.g., the endogenous agonist of the receptor). Factors affecting the precision of this assay and logical considerations associated with interpretation of the results are discussed in the Appendix.

The results of these and other assays with strychnine, brucine, and three *N*-substituted brucine analogues at the five muscarinic receptors (m1–m5) showed some clear patterns as well as a rather interesting lack of pattern. All the compounds showed similar patterns of subtype selectivity at [^{3}H]NMS-occupied (and free) receptors, with similar affinities at m1, m2, and m4 receptors and ~10-fold lower affinities at m3 and m5 receptors. Log affinity values of the three well characterized brucine analogues at unliganded m1 receptors ranged between 4.6 and 3.4.

In contrast to this consistent pattern with respect to affinity, the compounds showed very different patterns of allosteric interaction with [^{3}H]NMS and ACh across the receptor subtypes. Instances can be seen where an agent is negative with [^{3}H]NMS and positive with ACh; positive with [^{3}H]NMS and negative with ACh; negative with both ligands; or neutral with [^{3}H]NMS and positive, neutral, or negative with ACh. Some patterns can be seen with respect to cooperativity; at m2 receptors, these compounds show positive cooperativity with [^{3}H]NMS and negative cooperativity with ACh, and three of five compounds showed neutral or positive cooperativity with ACh at m3 receptors. Overall, however, each compound showed a unique pattern of cooperativity with respect to each primary ligand across the receptor subtypes, which presumably reflects the small differences in the effect of the chemical substitution on the affinity of the agent for the free and liganded receptor; a 2-fold difference in affinity in either direction is difficult to measure directly or predict, yet gives rise to the qualitatively different effects of positive or negative cooperativity. These results suggest that minor

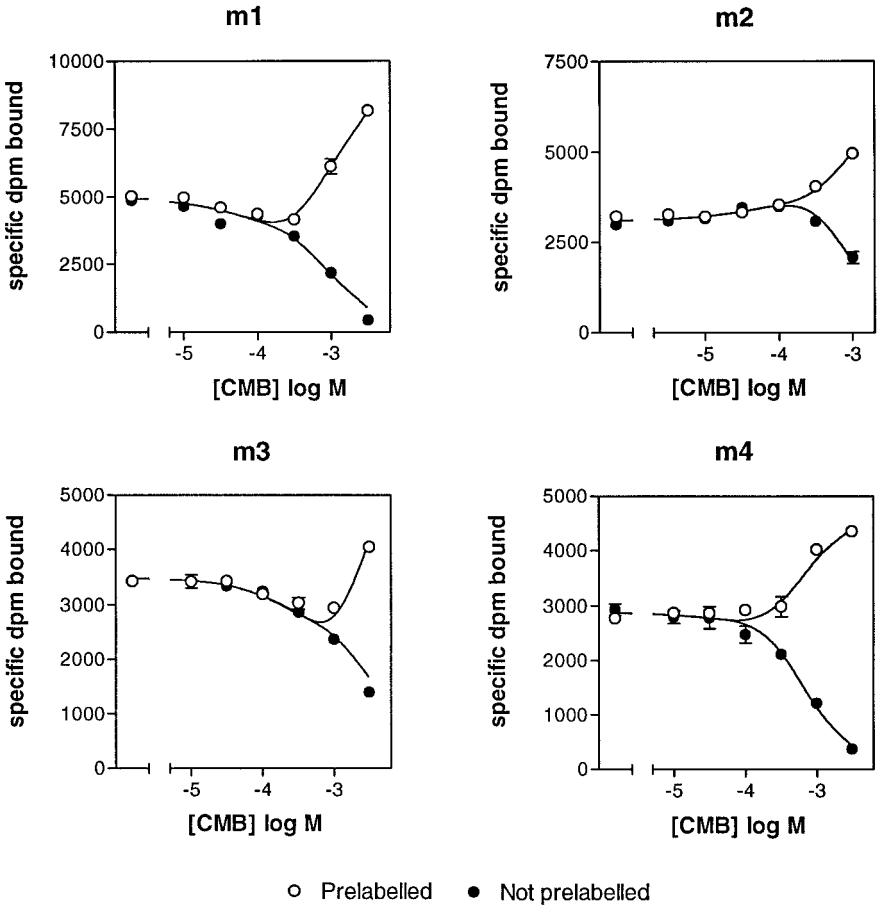

Fig. 4. Quantitative nonequilibrium assay with CMB. Receptors unlabeled or prelabeled with [^{3}H]NMS before the incubation with CMB. The final [^{3}H]NMS concentrations after dilution were 142, 280, 142, and 151 pM, and the incubation times were 90, 30, 95, and 67 min at m1–m4 receptors, respectively. Data are the mean and range/2 of duplicate measures from a single assay. *Lines*, fit to eq. 5. In the analysis of the data at m3 receptors, the K_d value of [^{3}H]NMS was fixed at 0.2 nM.

modification of a lead compound, showing low negative, neutral, or positive cooperativity with the endogenous ligand at one receptor subtype, may lead to the generation of a series of compounds with different patterns of cooperativity across the receptor subtypes. Most importantly for their therapeutic potential, such agents may show considerable subtype specificity, with regard to cooperativity rather than affinity (see below).

Brucine, BNO, and CMB were studied quantitatively using three different types of assay: (1) equilibrium [^{3}H]NMS binding with ACh, (2) [^{3}H]NMS dissociation, and (3) a nonequilibrium [^{3}H]NMS binding assay. The data were analyzed and interpreted using the ternary allosteric model of allosteric action, in which both the primary ligand and the allosteric agent can bind simultaneously to the receptor, and the binding of one type of ligand to the receptor alters the affinity of the other type of ligand. Overall, the internally consistent results provide support for the ternary allosteric model as the mechanism underlying the observed phenomena.

Although this model adequately accounts for the current data, some other, more complex, models also should be considered. For example, receptors may be considered to be free or coupled to G proteins and/or in inactive or active states, with agonists having higher affinity for the G protein-coupled receptor and/or for the active receptor state (Lefkowitz *et al.*, 1993). An allosteric agent might modulate agonist affinity differentially at the free and coupled receptor and/or at the inactive and active states. In addition, the allosteric agent may itself differentially recognize free/coupled and/or inactive/active receptor states. Such effects could lead to changes in both the efficacy and apparent affinity of the agonist. These more complex models may prove to be useful in future studies and may be required to account for the direct agonist-like effects observed with some allosteric agents (Jakubik *et al.*, 1996).

The fact that an allosteric agent can show neutral cooperativity with ACh suggests that allosteric agents may display a novel form of receptor subtype selectivity that we refer to as absolute subtype selectivity, which is in contrast to the relative selectivity shown by directly acting agonists and antagonists. A directly acting ligand may have relative selectivity for one receptor subtype by virtue of a higher affinity for that subtype: such selectivity must be large for it to be useful, both therapeutically and as a pharmacological tool. Nevertheless, however large the selectivity of the ligand, a sufficiently high concentration will occupy all the receptor subtypes. An allosteric agent that shows positive or negative cooperativity with the endogenous ligand at one subtype and neutral cooperativity at the other subtypes will show absolute selectivity. Such an agent will modulate the binding of the endogenous ligand at a single receptor while having no effect at the other receptors, even though the agent itself may bind to those other receptors. This selective action would be independent of both the magnitude of the positive or negative cooperativity at the single subtype and of the affinities of the agent for all the receptor subtypes, and selective action would be maintained regardless of the concentration of the allosteric agent.

Allosteric enhancers of endogenous ligand affinity are quite well known with respect to ion channel-coupled receptors [e.g., at $GABA_A$ receptors (Macdonald and Olsen, 1994),

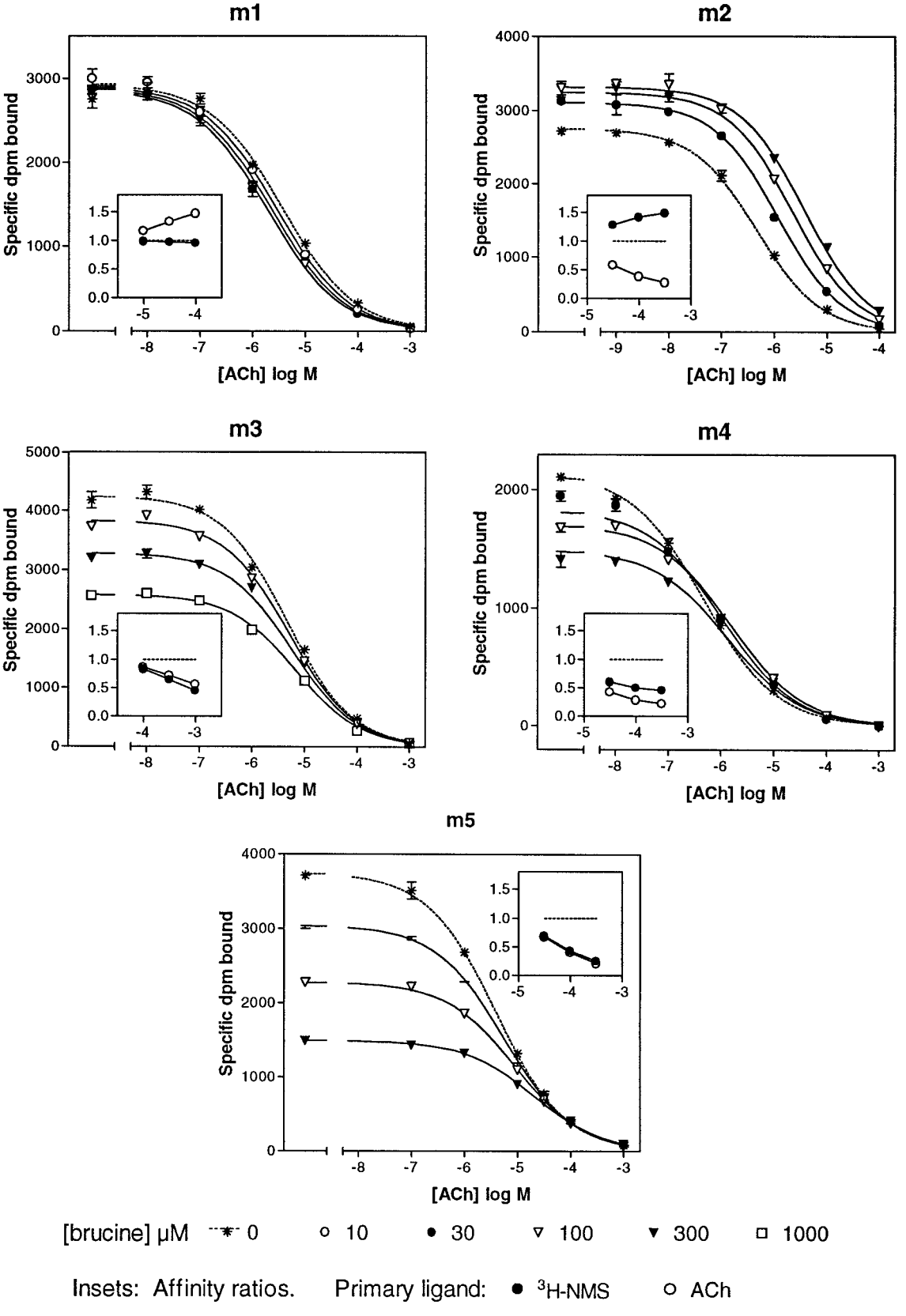

Fig. 5. Quantitative equilibrium assay with brucine. Binding of [^{3}H]NMS (0.2 nM for m1, m3, and m4 receptors; 0.4 nM for m2 receptors; 0.7 nM for m5 receptors) was measured, after a 3-hr incubation, alone and in the presence of six concentrations of ACh, alone, and in the presence of three concentrations of brucine. The data are the mean and range/2 of duplicate measures from a single assay. The data at m1, m2, m3, and m5 receptors were fitted to the equilibrium allosteric model (eq. 4 in Experimental Procedures) using nonlinear regression analysis. The data with m4 receptors were fitted to the nonequilibrium allosteric model (eq. 5) with the dissociation rate constant of [^{3}H]NMS set to 0.065 min^{-1}. *Insets*, affinity ratios [i.e., apparent affinity of the primary ligand ([^{3}H]NMS or ACh) in the presence of brucine divided by its affinity in the absence of brucine] derived from the values of the fitted parameters.

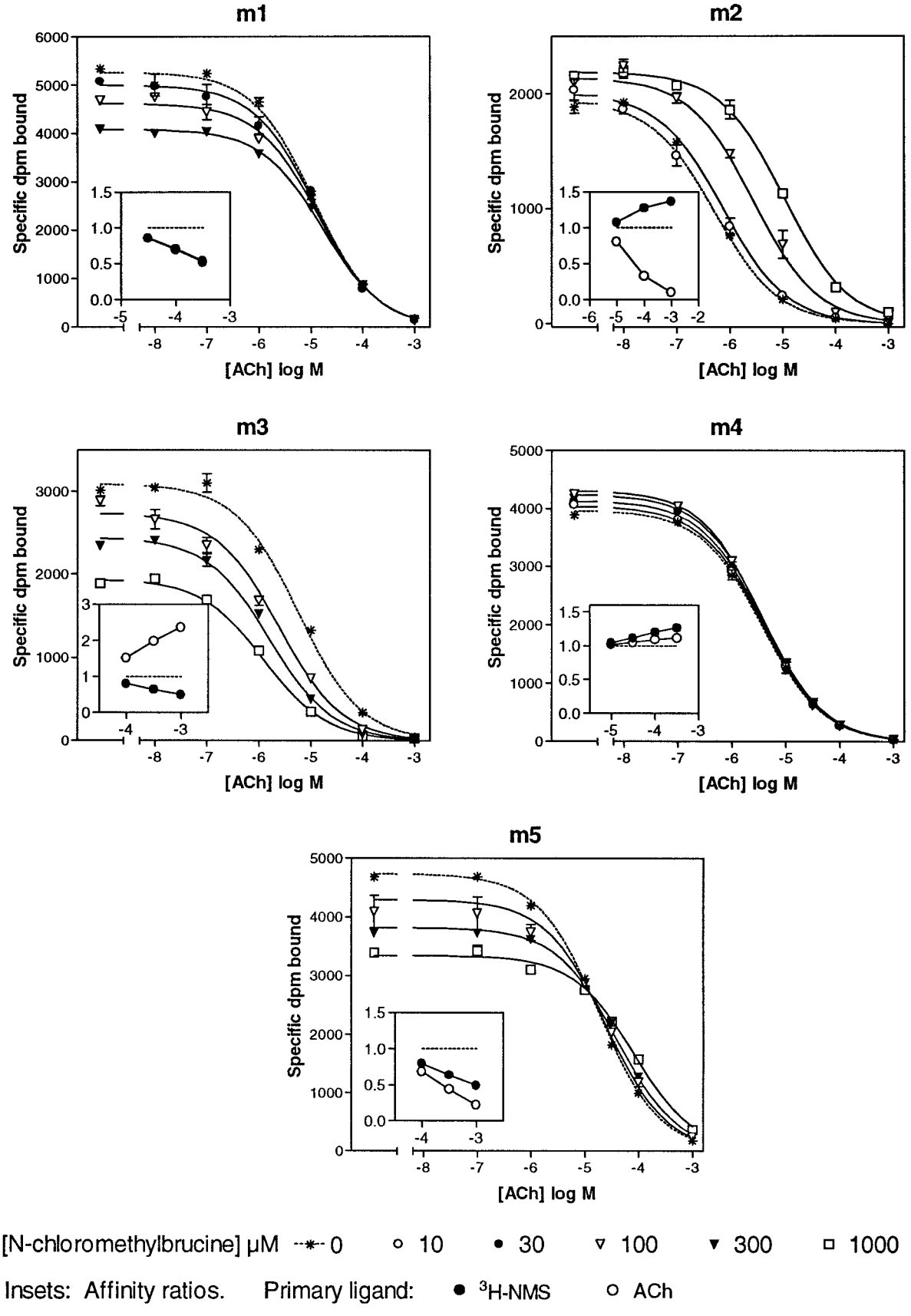

Fig. 6. Quantitative equilibrium assay with CMB. See legend to Fig. 5 for the experimental conditions. The data at m2 and m4 receptors were analyzed with eq. 5. At m2 receptors, the incubation time was 3 hr and the dissociation rate constant of [^{3}H]NMS was set to 0.337 min^{-1}. The data at m4 receptors were combined from four assays (240 data points) conducted on the same day with different ranges of [CMB] and incubation times of 2.5 and 5 hr; the dissociation rate constant of [^{3}H]NMS was set to 0.065 min^{-1}.

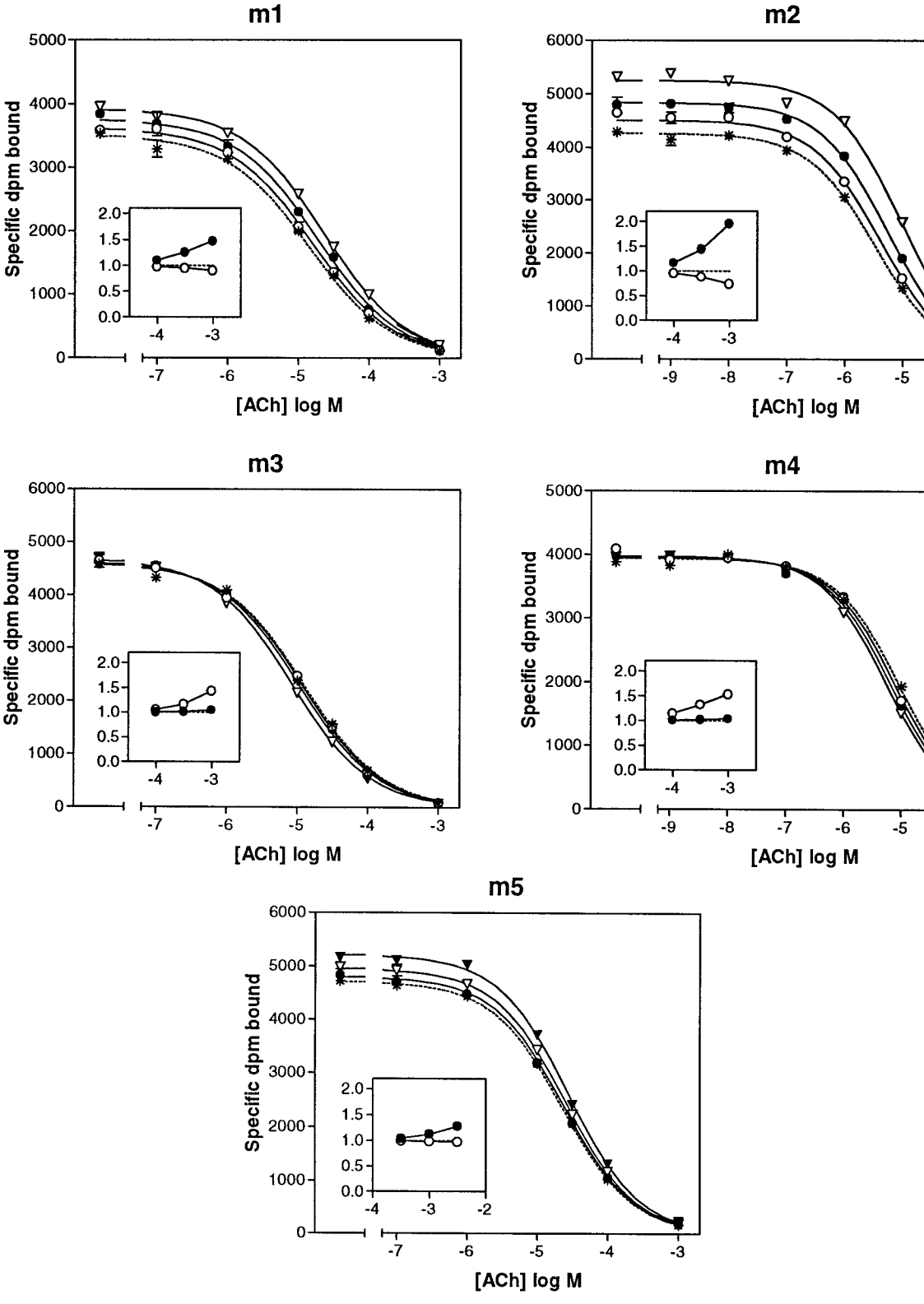

Fig. 7. Quantitative equilibrium assay with BNO. See legend to Fig. 5 for the experimental conditions.

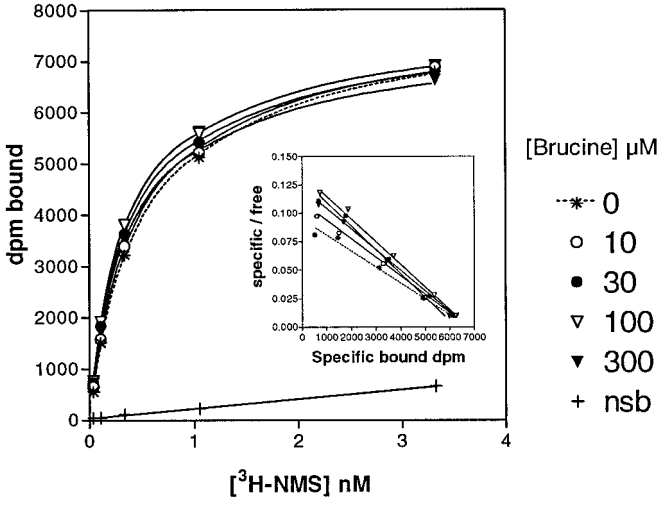

Fig. 8. Saturation binding curves of [^{3}H]NMS at m2 receptors in the presence of various concentrations of brucine. A 3-hr incubation time was used. The data are mean of duplicate measures obtained in a single assay. Nonspecific binding was not affected by brucine (data not shown) and was measured here in the absence of brucine. The data were fitted to the allosteric model, with the value of B_{max} shared between all curves except in the presence of 0.3 mM brucine. To obtain well defined parameter estimates in this and similar experiments, it was necessary to fix the value of the log affinity of brucine at the [^{3}H]NMS-occupied m2 receptor to 4.59, the value obtained (±0.02) from five off-rate assays.

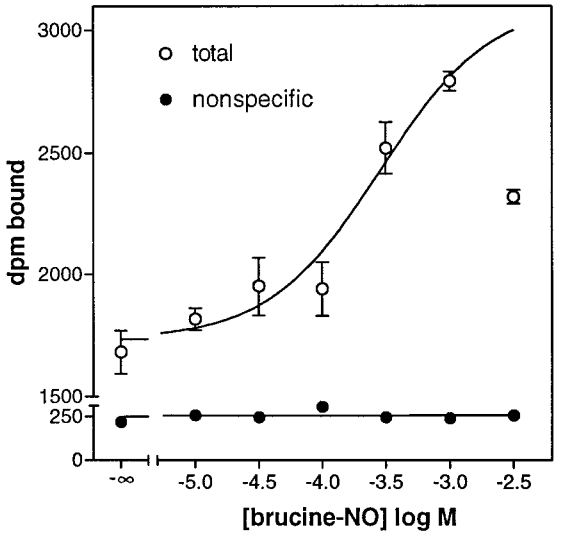

Fig. 9. Effect of BNO on [^{3}H]ACh binding to m4 receptors. [^{3}H]ACh (8 nM) was incubated with various concentrations of BNO for 1 hr at 30°. Data are the mean ± standard error of triplicate measures for total binding and single measures of nonspecific binding. The data were fitted to a hyperbolic function to estimate the EC_{50} value and maximal effect. The data point with 3 mM BNO was not included in the analysis. Inhibitory effects of BNO concentrations of >1 mM were seen in two other assays. In this assay, BNO increased binding by 93% with a $-\log EC_{50}$ of 3.6. [^{3}H]ACh has a K_d value of 24 ± 6 nM (six experiments) at m4 receptors.

N-methyl-D-aspartate receptors (Hollmann and Heinemann, 1994), strychnine-sensitive glycine receptors (Mascia *et al.*, 1996), P2X purinoceptors (Pintor *et al.*, 1996), and nicotinic cholinergic receptors (Schrattenholz *et al.*, 1996)]. Among G protein-coupled receptors, only the adenosine A_1 receptor is known to have an allosteric site that supports positive cooperativity with the endogenous ligand (Kollias-Baker *et al.*, 1994). The current finding of positive cooperativity with the endogenous ligand at muscarinic receptors raises the possibility that other G protein-coupled receptors, perhaps including α_2-adrenergic, dopamine D_2, and 5- hydroxytryptamine$_{1B/1D}$ receptors (Nunnari *et al.*, 1987; Hoare and Strange, 1996; Massot *et al.*, 1996), also may have such allosteric sites. Agents that are positively cooperative with the endogenous ligand might not be detected by most screening assays involving interactions with radiolabeled antagonists or action at the receptors in the absence of endogenous ligand. Because G protein-coupled receptors are the targets of many therapeutically effective drugs, the presence of allosteric sites on these receptors might allow the development of drugs with novel modes of action at known therapeutic targets.

In conclusion, brucine and some *N*-substituted analogs have been shown to enhance allosterically the affinity of ACh at muscarinic receptors by up to ~3-fold. Each compound showed a different pattern of cooperative interactions with ACh and [^{3}H]NMS across the receptor subtypes. In addition to positive and negative cooperative effects, in some cases the brucine analogues displayed neutral cooperativity with ACh (i.e., the analogue bound to the receptor but did not affect the affinity of ACh). An allosteric agent with positive or negative cooperativity with the endogenous ligand at one receptor subtype and neutral cooperativity at the other subtypes would have absolute subtype selectivity. The current findings suggest that it may be possible to develop highly receptor subtype-selective agents showing various patterns of cooperativity with the endogenous ligand across a range of receptor subtypes.

Appendix: Affinity Ratio Assay

The design of radioligand binding assays to screen for ligands that are competitive with the endogenous ligand is relatively straightforward because it can be assumed that the test agent will have the same effect on the binding of the endogenous ligand as it had on the binding of the radioligand. An allosteric agent, however, could well have different effects on the binding of different primary ligands, so screening assays must measure allosteric effects with the unlabeled endogenous ligand in competition with a radioligand and therefore are more complex. Quantitative results can be obtained from an assay that measures the effect of a range of concentrations of allosteric agent, each in the presence of a range of concentrations of the endogenous ligand, on the binding of a single concentration of radioligand, but this design is inefficient if accurate quantitative data are not required. The allosteric effect on the unlabeled ligand also may not be visualized easily against the background of the allosteric effect on the radioligand, so the assay requires relatively complex nonlinear regression analysis. For our experiments, the requirements were (1) an efficient assay that measured the effect of the test agent on the binding of a single concentration of radioligand in the absence and presence of a single concentration of unlabeled ligand, (2) that the effects of the test agent on the binding of the labeled and unlabeled ligands be displayed using a common measure, and (3) for simplicity that the results be calculated rather than estimated with nonlinear regression.

The semiquantitative equilibrium assay we devised (Lazareno and Birdsall, 1995) (the affinity ratio assay) has these properties, and the common measure used to express the effects of the test agent on the labeled and unlabeled ligands is the affinity ratio (i.e., the apparent affinity of the primary ligand in the presence of test agent alone divided by its true

TABLE 4
Parameters for the interaction of CMB with [^{3}H]NMS and ACh at m1—m5 muscarinic receptors

Subtype	Assay	Log affinity		Cooperativity		n
		Unoccupied receptor	[^{3}H]NMS-occupied receptor	[^{3}H]NMS	ACh	
m1	Nonequilibrium	4.44 ± 0.08	4.23 ± 0.11	0.63 ± 0.04		3
	Equilibrium	4.38 ± 4.10	4.10 ± 0.20	0.54 ± 0.07	0.45 ± 0.05	4
m2	Nonequilibrium	4.28 ± 0.03	4.41 ± 0.01	1.36 ± 0.09		2
	Equilibrium	4.22 ± 0.11	4.37 ± 0.12	1.38 ± 0.03	0.094 ± 0.019	4
m3	Nonequilibrium	3.71 ± 0.03	3.42 ± 0.02	0.52 ± 0.01		3
	Equilibrium	3.66 ± 0.13	3.26 ± 0.23	0.43 ± 0.11	3.26 ± 0.23	4
m4	Nonequilibrium	4.29 ± 0.04	4.32 ± 0.05	1.08 ± 0.14		3
	Equilibrium	4.32 ± 0.03	4.32 ± 0.08[a]	1.08 ± 0.09	1.03 ± 0.14	4
m5	Nonequilibrium					
	Equilibrium	3.66 ± 0.04	3.26 ± 0.04	0.40 ± 0.01	0.055 ± 0.010	2

[a] n = 2, log affinity at the [^{3}H]NMS-occupied receptor was fixed at 4.37 in two assays.

TABLE 5
Parameters for the interaction of BNO with [^{3}H]NMS and ACh at m1—m5 muscarinic receptors

Subtype	Assay	Log affinity		Cooperativity		n
		Unoccupied receptor	[^{3}H]NMS-occupied receptor	[^{3}H]NMS	ACh	
m1	Nonequilibrium	3.37 ± 0.08	3.53 ± 0.10	1.47 ± 0.10		3
	Equilibrium	3.39 ± 0.11	3.57 ± 0.13	1.56 ± 0.20	0.96 ± 0.17	4
m2	Nonequilibrium	3.13 ± 0.04	3.32 ± 0.03	1.55 ± 0.04		2
	Equilibrium	2.68 ± 0.12	3.25 ± 0.09	3.75 ± 0.40	0.43 ± 0.20	4
m3	Nonequilibrium	2.79 ± 0.09	2.82 ± 0.10	1.06 ± 0.02		3
	Equilibrium	2.73 ± 0.16	2.89 ± 0.15[a]	1.16 ± 0.08	2.60 ± 0.20	4
m4	Nonequilibrium	3.68 ± 0.03	3.67 ± 0.08	0.98 ± 0.11		3
	Equilibrium	3.46 ± 0.11	3.47 ± 0.06[b]	0.91 ± 0.09	1.42 ± 0.12[c]	4
m5	Nonequilibrium					
	Equilibrium	2.45 ± 0.07	2.65 ± 0.05	1.60 ± 0.08	0.78 ± 0.17	2

[a] n = 3, log affinity at the [^{3}H]NMS-occupied receptor was fixed at 2.5 in one assay.
[b] n = 3, log affinity at the [^{3}H]NMS-occupied receptor was fixed at 3.6 in one assay.
[c] Significantly different from 1, $p < 0.05$, two-tailed t test.

TABLE 6
Parameters for the interaction of strychnine with [^{3}H]NMS and ACh at m1—m5 muscarinic receptors

Subtype	Assay	Log affinity		Cooperativity		n
		Unoccupied receptor	[^{3}H]NMS-occupied receptor	[^{3}H]NMS	ACh	
m1	Nonequilibrium	5.13	5.00	0.8	0.32	
	Equilibrium	4.90	4.90	1.0	0.41	
m2	Nonequilibrium	4.86	5.24	2.4	0.05	
	Equilibrium	4.96	5.28	2.2	0.15	
m3	Nonequilibrium					
	Equilibrium	4.16	4.02	0.7	<0.1	
m4	Nonequilibrium	4.78	5.07	1.8	0.14	
	Equilibrium	5.01	5.23	1.7	0.46	
m5	Nonequilibrium					
	Equilibrium	3.87 ± 0.05	3.05 ± 0.04	0.15 ± 0.01	<0.01	2

Values at m1—m4 receptors are from Lazareno and Birdsall (1995).

affinity measured in the absence of test agent). This measure is novel as far as we are aware and is identical formally to the reciprocal of the dose ratio measured in assays from which Schild plots are derived. We refer to the affinity ratio assay as semiquantitative because it allows approximate estimates to be made of the affinity of the test agent and its allosteric effects on the labeled and unlabeled ligands. This is achieved through visual inspection of the affinity ratio plots together with a logical consideration of the affinity ratio data in conjunction with the results of off-rate assays that measure the kinetic effects of the agent on radioligand dissociation. The logic assumes that the equilibrium and kinetic effects of the agent can be related to each other by the ternary allosteric model, in which the primary and allosteric ligands can bind simultaneously to the receptor and reciprocally affect the affinity of each other for the receptor (Lazareno and Birdsall, 1995).

In this appendix, we address four issues: (1) the theoretical effect on the value of the affinity ratio when the unlabeled ligand binds with a slope factor different from unity, (2) the variability of the assay, both within a single assay and between assays, (3) effects on the observed affinity ratios of the slowing of radioligand binding by high concentrations of allosteric agent, and (4) the logic with which the affinity ratio assay is interpreted in conjunction with the results from off-rate assays.

Effect of the Slope Factor of the Unlabeled Ligand on the Affinity Ratio

We demonstrated previously that the fractional effect of a particular concentration of allosteric agent on the affinity ratio of both the labeled and unlabeled ligands is independent of the concentrations of primary ligands and corresponds to the fractional occupancy by the allosteric agent of

the free receptor. The affinity ratio plot therefore has an EC_{50} or IC_{50} value corresponding to the K_d value of the allosteric agent and an asymptote corresponding to the cooperativity between the primary and allosteric ligands. These properties were derived with the assumption that both labeled and unlabeled ligands bound according to the law of mass action [i.e., with Hill slope factors of 1 (Lazareno and Birdsall, 1995)]. In practice, however, unlabeled agonists often inhibit radioligand binding with slopes of <1, even in the presence of GTP, and it is necessary to introduce an empirical slope factor into the mechanistic model used to analyze detailed assays with nonlinear regression. Here we show that the affinity ratio value calculated in the affinity ratio assay using a single concentration of unlabeled ligand is independent of the slope factor describing the binding of the unlabeled ligand.

In the ternary allosteric model, a receptor, R, has a binding site for a primary ligand, which is either a radioligand, L, or an unlabeled competitor, A, and a second binding site for an allosteric ligand, X. K_L, K_A, and K_X are affinity constants for binding of the receptor with L, A, and X, respectively; and α and β are the allosteric constants of X with L and A, respectively (i.e., the affinity of L for the X-occupied receptor is $\alpha{\cdot}K_L$ and the affinity of X for the L-occupied receptor is $\alpha{\cdot}K_X$, and similarly with A, K_A, and β). A binds to R with a slope factor of n, and the receptor concentration is B_{max}.

The specific binding of the radioligand in the presence of X is given by

$$B_{LX} = \frac{B_{max}\cdot L{\cdot}K_L\cdot(1+\alpha\cdot X\cdot K_X)}{1+X\cdot K_X+L\cdot K_L\cdot(1+\alpha\cdot X\cdot K_X)} \quad (7)$$

The specific binding of the radioligand in the presence of A and X, B_{LAX}, is given by

$$B_{LAX} = \frac{B_{max}\cdot L\cdot K_L\cdot(1+\alpha\cdot X\cdot K_X)}{1+X\cdot K_X+(A\cdot K_A)^n(1+\beta\cdot X\cdot K_X)+L\cdot K_L\cdot(1+\alpha\cdot X\cdot K_X)} \quad (8)$$

The apparent affinity of A in the presence of X, K_{AX}, is calculated as

$$K_{AX} = \frac{B_{max}\cdot(B_{LX}-B_{LAX})}{A\cdot B_{LAX}\cdot(B_{max}-B_{LX})} \quad (9)$$

By substituting eqs. 7 and 8 into eq. 9, the apparent affinity of A in the presence of X is

$$K_{AX} = \frac{1+\beta\cdot X\cdot K_X}{1+X\cdot K_X}\cdot A^{(n-1)}\cdot K_A^n \quad (10)$$

and the apparent affinity of A in the absence of X is

$$K_A = A^{(n-1)}\cdot K_A^n \quad (11)$$

The apparent affinity of A, which is measured with a single concentration of A, in both the absence and presence of X, therefore is a function of both [A] and n, as well as K_A. The affinity ratio, however, is independent of [A] and n

$$\text{Affinity ratio of A} = \frac{K_{AX}}{K_A} = \frac{1+\beta\cdot X\cdot K_X}{1+X\cdot K_X} \quad (12)$$

Variability in the Affinity Ratio Assay

Within-assay variability. Affinity ratios are calculated from a number of mean values, each measured with some degree of experimental error. It is useful to be able to see the standard error (square root of the variance) of calculated affinity ratios displayed on the affinity ratio plot, as shown in Fig. 2. This is achieved using the equation

$$\text{var}[f(\nu_1,\ \nu_2 \ldots\ \nu_m)] \approx \sum_{i=1}^{m}\left[\text{var}(\nu_i)\cdot\left(\frac{\partial f}{\partial \nu_i}\right)^2\right] \quad (13)$$

That is, the variance of a function of uncorrelated variables is approximately equal to the sum of the products of the variance of each variable and the square of the partial differential of the function (Colquhoun, 1971). The variables used to calculate the affinity ratios, r_L and r_A, of the labeled and unlabeled ligand, respectively, are the mean values of specific radioligand binding alone, in the presence of test agent, unlabeled ligand, test agent plus unlabeled ligand, and a high concentration of radioligand alone, represented by L, X, A, Y, and H, respectively. The symbol q represents the ratio of the low and high concentrations of radioligand and is treated as a constant. For simplicity, the variability of nonspecific binding also is ignored. The equations defining r_L and r_A are

$$r_L = \frac{X\cdot(H-L)}{H\cdot L\cdot(1-q)-X\cdot(L-q\cdot H)} \quad (14)$$

$$r_A = \frac{L\cdot A\cdot(H-L)(X-Y)}{Y\cdot(L-A)\cdot[H\cdot L\cdot(1-q)-X\cdot(L-q\cdot H)]} \quad (15)$$

The partial differential equations are

$$\frac{\partial r_L}{\partial L} = -\frac{H\cdot X\cdot(H-X)\cdot(1-q)}{[H\cdot L\cdot(1-q)-X\cdot(L-q\cdot H)]^2} \quad (16)$$

$$\frac{\partial r_L}{\partial H} = \frac{L\cdot X\cdot(L-X)\cdot(1-q)}{[H\cdot L\cdot(1-q)-X\cdot(L-q\cdot H)]^2} \quad (17)$$

$$\frac{\partial r_L}{\partial X} = \frac{H\cdot L\cdot(H-L)\cdot(1-q)}{[H\cdot L\cdot(1-q)-X\cdot(L-q\cdot H)]^2} \quad (18)$$

$$\frac{\partial r_A}{\partial L} = -\frac{A\cdot(X-Y)\cdot\{H\cdot L^2\cdot(1-q)\cdot(H-X-A)+A\cdot X\cdot[L\cdot(L-q\cdot H)+q\cdot H\cdot(H-L)]\}}{Y\cdot(L-A)^2\cdot[H\cdot L\cdot(1-q)-X\cdot(L-q\cdot H)]^2} \quad (19)$$

$$\frac{\partial r_A}{\partial H} = \frac{L^2\cdot A\cdot(X-Y)\cdot(1-q)\cdot(L-X)}{Y\cdot(L-A)\cdot[H\cdot L\cdot(1-q)-X\cdot(L-q\cdot H)]^2} \quad (20)$$

$$\frac{\partial r_A}{\partial X} = \frac{L\cdot A\cdot(H-L)\cdot(L\cdot H\cdot(1-q)-Y\cdot(L-q\cdot H))}{Y\cdot(L-A)\cdot[H\cdot L\cdot(1-q)-X\cdot(L-q\cdot H)]^2} \quad (21)$$

$$\frac{\partial r_A}{\partial A} = \frac{L^2\cdot(H-L)\cdot(X-Y)}{Y\cdot(L-A)^2\cdot[H\cdot L\cdot(1-q)-X\cdot(L-q\cdot H)]} \quad (22)$$

$$\frac{\partial r_A}{\partial Y} = -\frac{L\cdot A\cdot X\cdot(H-L)}{Y^2\cdot(L-A)\cdot[H\cdot L\cdot(1-q)-X\cdot(L-q\cdot H)]} \quad (23)$$

These partial differentials, together with the experimentally measured variances of each variable, are inserted into eq. 13 to obtain an overall estimate of the variance associated with the calculated affinity ratios.

The affinity ratio assay also may be conducted without using a high concentration of radioligand but assuming a specified value for the affinity of the radioligand. In this protocol, the symbol p represents the product of radioligand

concentration and affinity. The equations defining r_L and r_A are

$$r_L = \frac{X}{L \cdot (p + 1) - p \cdot X} \quad (24)$$

$$r_A = \frac{L \cdot A \cdot (X - Y)}{Y \cdot (L - A) \cdot [L \cdot (p + 1) - p \cdot X]} \quad (25)$$

The partial differential equations are

$$\frac{\partial r_L}{\partial L} = -\frac{X \cdot (p + 1)}{[L \cdot (p + 1) - p \cdot X]^2} \quad (26)$$

$$\frac{\partial r_L}{\partial X} = \frac{L \cdot (p + 1)}{[L \cdot (p + 1) - p \cdot X]^2} \quad (27)$$

$$\frac{\partial r_A}{\partial L} = -\frac{A \cdot (X - Y) \cdot [L^2 \cdot (p + 1) - p \cdot A \cdot X]}{Y \cdot (L - A)^2 \cdot [L \cdot (p + 1) - p \cdot X]^2} \quad (28)$$

$$\frac{\partial r_A}{\partial X} = \frac{L \cdot A \cdot [L \cdot (p + 1) - p \cdot Y]}{Y \cdot (L - A) \cdot [L \cdot (p + 1) - p \cdot X]^2} \quad (29)$$

$$\frac{\partial r_A}{\partial A} = \frac{L^2 \cdot (X - Y)}{Y \cdot (L - A)^2 \cdot [L \cdot (p + 1) - p \cdot X]} \quad (30)$$

$$\frac{\partial r_A}{\partial Y} = -\frac{L \cdot A \cdot X}{Y^2 \cdot (L - A) \cdot [L \cdot (p + 1) - p \cdot X]} \quad (31)$$

The variances of the affinity ratios can be estimated using eq. 13.

Between-assay variability. As a screening assay, useful semiquantitative results should be obtained from a single assay using a limited range of concentrations of test agent. It therefore is important to assess the precision with which affinity ratios can be measured. The between-assay variability was assessed theoretically and experimentally.

Specific binding data from affinity ratio assays were simulated, in duplicate, with random error with a normal distribution and a standard deviation of 3%, the size of variability between duplicates that occurs typically in our assays. Fig. 10A shows affinity ratio plots obtained with various combinations of cooperativity values for the labeled and unlabeled ligands. The curves in each panel were derived from 100 simulated assays, and the error bars represent the standard deviation. The variability of the affinity ratio is related directly to its magnitude, and the variability of the affinity ratio of the unlabeled ligand is greater than that of the labeled ligand. With affinity ratios of <1, the points are sufficiently well defined to allow reasonable estimates of the IC_{50} value, even with data from the unlabeled ligand. The simulation did not take into account variation in nonspecific binding and background radiation, which can lead to a larger variability in the affinity ratio of the unlabeled ligand when radioligand binding is inhibited strongly (data not shown). The variability of affinity ratios of >1 depends on the concentration of radioligand, with concentrations below the K_d value providing the best precision (data not shown).

The consistency of affinity ratio plots across assays was confirmed experimentally. Fig. 11 shows combined data from four assays measuring affinity ratios of [^{3}H]NMS and four agonists in the presence of CMB at m2 receptors. CMB was positive with [^{3}H]NMS and negative with ACh, as observed earlier; it also was negative with carbachol, slightly negative with oxotremorine, and neutral with pilocarpine. The standard errors derived from affinity ratios from four assays were small, as predicted with the simulations, and were similar to or smaller than the within-assay estimated standard errors (data not shown), except for oxotremorine, which in one assay showed the same pattern as in the other assays but displaced toward 1. In summary, the calculated within-assay standard error gives a reasonable impression of the reliability of the data, and the value of individual affinity ratios is consistent between assays.

Theoretical effects of kinetic artifacts in the affinity ratio assay. Most ligands acting allosterically at muscarinic receptors almost completely slow the dissociation of [^{3}H]NMS at high concentrations. Negatively cooperative agents inhibit [^{3}H]NMS binding at lower concentrations than are needed to observe the effects on [^{3}H]NMS kinetics. Agents that are neutral or positively cooperative with [^{3}H]NMS, however, will exert kinetic-slowing effects on [^{3}H]NMS association in the same concentration range in which equilibrium effects are observed. If the agent slows the kinetics of [^{3}H]NMS sufficiently, then binding equilibrium will not be achieved and the resulting inhibition of [^{3}H]NMS binding will be a kinetic artifact, rather than a reflection of competition or negative cooperativity. We investigated the effect of kinetic artifacts on the observed affinity ratios of labeled and unlabeled ligands using simulation.

Fig. 10B shows affinity ratios calculated from binding data simulated using eq. 5. The dissociation rate constant of [^{3}H]NMS was set to 0.03 min^{-1}, and the incubation time was set to 120 min. Affinity ratios were obtained with [^{3}H]NMS (*closed symbols*) and ACh (*open symbols*); shown are observed results (*triangles*) and values that would have been observed at equilibrium (*circles*). As expected, kinetic artifacts with [^{3}H]NMS are larger and occur at lower concentrations as the cooperativity of the allosteric agent with [^{3}H]NMS increases. Even with (negative) cooperativity with [^{3}H]NMS of 0.5, kinetic artifacts occur with concentrations of allosteric agent 10-fold greater than its K_d value; artifacts occur with even lower concentrations if there is positive cooperativity with ACh. Kinetic artifacts with [^{3}H]NMS cause an artifactual increase in the affinity ratio of ACh, which rises with increasing concentrations of allosteric agent to a maximum and then declines. The size of this artifact increases as the cooperativity with both [^{3}H]NMS and ACh increases.

Interpretation of the results of an affinity ratio assay in conjunction with those of an off-rate assay. If the test agent acts allosterically according to the ternary allosteric model, then the results of the affinity ratio and off-rate assays reflect different aspects of the same interaction. Although the off-rate assay provides a quantitative estimate of a single parameter, the IC_{50} values, the affinity ratio assay provides semiquantitative estimates of four parameters: the EC_{50} and/or IC_{50} values and the direction and magnitude of cooperativity with [^{3}H]NMS and ACh. The objective is to construct a scenario that is consistent with both sets of results given the following constraints: the IC_{50} value of the agent in the off-rate assay corresponds to the K_d value of the agent for the [^{3}H]NMS-occupied receptor; the IC_{50} or EC_{50} values in the affinity ratio assay with both [^{3}H]NMS and ACh correspond approximately to the K_d value of the agent at the free receptor; the ratio of the K_d values of the agent at the

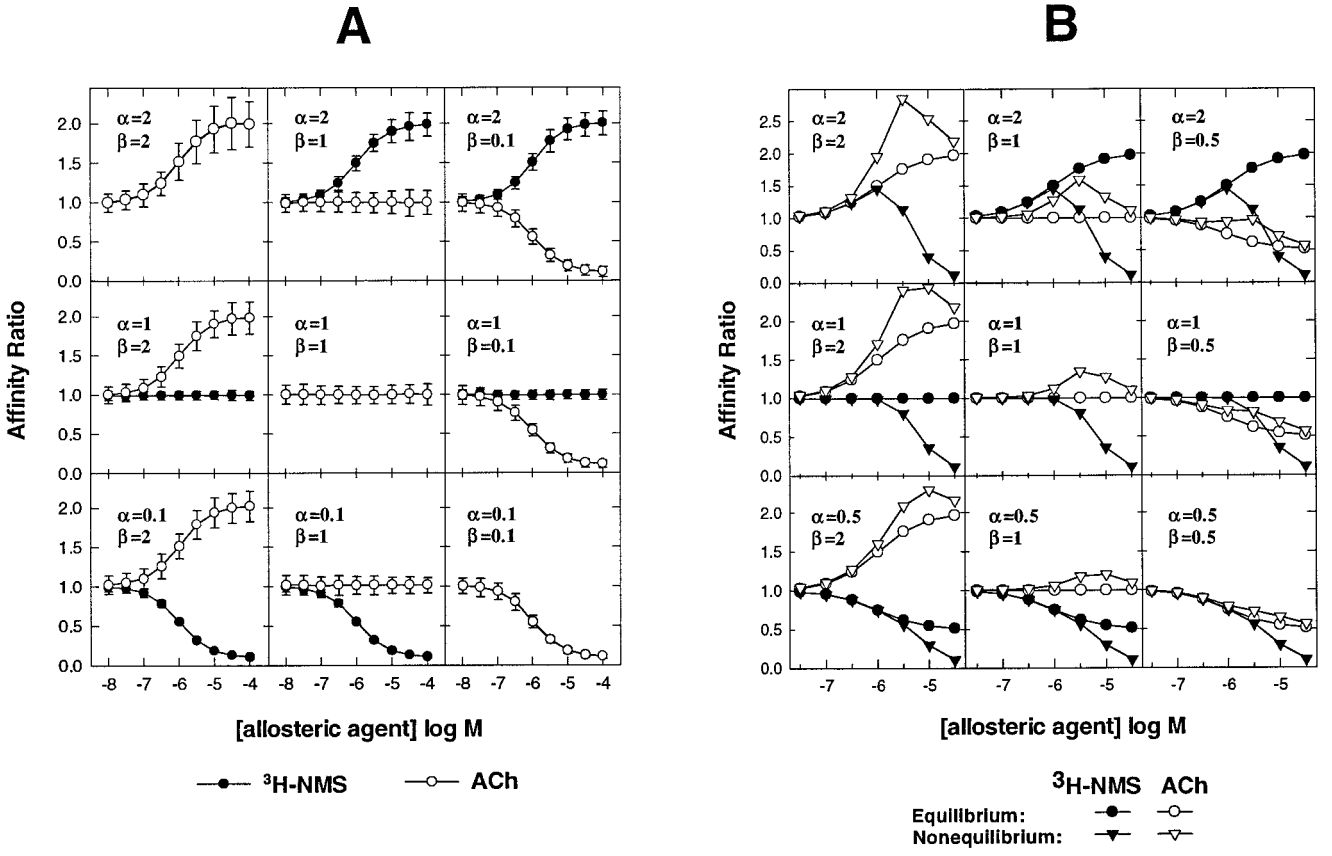

Fig. 10. Affinity ratio values calculated from simulated data. A, Predicted variability of affinity ratios. Data corresponding to specific binding data obtained empirically in an affinity ratio assay were generated using eq. 4, and normally distributed error with a standard deviation of 3% was added. Affinity ratios were calculated using eqs. 1–3. The radioligand concentration was set to the K_d value, the fixed concentration of unlabeled ligand was the IC_{50} value, and the affinity of the allosteric agent for the free receptor was 10^6 M^{-1}. Data are the mean and standard deviation of 100 curves. Where the cooperativity with labeled (α) and unlabeled (β) ligands is the same, only data of the unlabeled ligand are shown. B, Predicted kinetic artifacts when high concentrations of allosteric agent prevent radioligand binding from reaching equilibrium. Data corresponding to specific binding data obtained empirically in an affinity ratio assay were generated using eq. 5. The radioligand concentration was twice the K_d value; the concentration of unlabeled ligand was the IC_{50}; the affinity of the allosteric agent for the free receptor was 10^6 M^{-1}; the dissociation rate constant of [^{3}H]NMS was 0.03 min^{-1}; and the incubation time was 2 hr.

free and [^{3}H]NMS-occupied receptor correspond to the cooperativity of the agent with [^{3}H]NMS, which should be consistent with the cooperativity observed in the affinity ratio assay; and kinetic artifacts will occur with concentrations of agent that increase the half-time for [^{3}H]NMS dissociation to ≥50 min (given an incubation time of 120 min and a K_d concentration of [^{3}H]NMS). The logic for analyzing the results is illustrated using data with *N*-benzyl brucine at m2 and m3 receptors (Figs. 2B and 3 and Table 1); the results shown in Table 1 with benzyl brucine are scenarios consistent with the data from at least two affinity ratio assays.

Based on the off-rate assay with m2 receptors, *N*-benzyl brucine has a log affinity of 4.8 for the [^{3}H]NMS-occupied receptor, so kinetic artifacts are not expected with concentrations of <0.4 mM (given a [^{3}H]NMS dissociation half-time of 2 min from the m2 receptor). *N*-Benzyl brucine reduces ACh affinity by 50% at a −log concentration of ~4.4, so this is an estimate of its log affinity for the free receptor. *N*-Benzyl brucine is positively cooperative with [^{3}H]NMS and has a log affinity of 4.8 at the [^{3}H]NMS-occupied receptor, so its affinity at the free receptor must be <4.8, which is consistent with the affinity of 4.4 estimated on the basis of its inhibitory potency. The estimated difference in affinity is 0.4 log units (2–3-fold), which agrees with the observed affinity ratio value of 2.5 with [^{3}H]NMS in the presence of 10^{-4} M *N*-benzyl brucine. The cooperativity with [^{3}H]NMS at m2 receptors therefore is shown as ++ in Table 1. Inspection of the graph (Fig. 2B, m2 data) suggests that the asymptotic level of inhibition of ACh affinity is >0, which implies that *N*-benzyl brucine has low negative cooperativity with ACh. This cooperative interaction is shown symbolically as − in Table 1. The fractional inhibition of the binding of a low concentration of [^{3}H]ACh by *N*-benzyl brucine at m2 receptors was very similar to its effect on the affinity ratio of unlabeled ACh in terms of both IC_{50} value and the asymptotic level of inhibition, suggesting that the cooperative effect of *N*-benzyl brucine on ACh binding is similar at free and G protein-coupled m2 receptors.

At m3 receptors, *N*-benzyl brucine inhibits [^{3}H]NMS binding by 50% at a -log concentration of ~3.8. Because its log affinity at the [^{3}H]NMS-occupied receptor also is 3.8, the inhibition reflects negative cooperativity rather than a kinetic artifact; at a log concentration of −3.8, the binding kinetics of [^{3}H]NMS would be only ~2-fold slower, and binding equilibrium would be attained. The negative cooperativity of *N*-benzyl brucine with [^{3}H]NMS, however, indicates that its affinity for the free receptor must be >3.8. This discrepancy can be accounted for if *N*-benzyl brucine has low

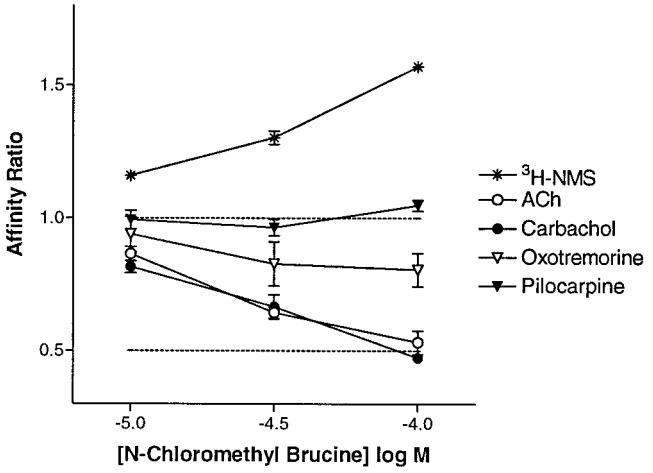

Fig. 11. Allosteric effects of CMB on [^{3}H]NMS, ACh, carbachol, oxotremorine, and pilocarpine binding at m2 receptors. Data are the mean and standard error from four affinity ratio assays. The [^{3}H]NMS concentration was 0.41 nM, and the concentrations of unlabeled ligands were 2, 10, 1, and 10 μM, respectively. The observed K_d value of [^{3}H]NMS was 0.41 ± 0.01 nM, and the observed log affinities of the unlabeled ligands were 5.81 ± 0.02, 5.22 ± 0.03, 6.25 ± 0.04, and 5.40 ± 0.01, respectively. The incubation time was 1 hr.

negative cooperativity with [^{3}H]NMS and an asymptotic level of inhibition >0, which would cause the true IC_{50} value (i.e., K_d) to be less than the concentration that reduced [^{3}H]NMS affinity by 50%. This conclusion is reflected in the symbolic value of − in Table 1. *N*-Benzyl brucine increased the affinity ratio of ACh at m3 receptors by 1.7-fold at a log concentration of −4. Given the uncertainty concerning the affinity of *N*-benzyl brucine at m3 receptors and the accuracy of the affinity ratio data, it is not possible to predict the affinity ratio of ACh at concentrations of *N*-benzyl brucine of $>10^{-4}$ M, so the symbol + is used in Table 1 to describe the positive cooperativity between *N*-benzyl brucine and ACh at m3 receptors, corresponding to the affinity ratio of 1.7 observed with the highest concentration used.

Acknowledgments

We thank Gareth Birdsall for helpful discussions regarding the evaluation of errors associated with the affinity ratio assay.

References

Birdsall NJM, Farries T, Gharagozloo P, Kobayashi S, Kuonen D, Lazareno S, Popham A, and Sugimoto M (1997) Selective allosteric enhancement of the binding and actions of acetylcholine at muscarinic receptor subtypes. *Life Sci* **60:**1047–1052.
Birdsall NJM and Hulme EC (1989) The binding properties of muscarinic receptors, in *The Muscarinic Receptors* (Brown JH, ed) pp 31–92, Humana Press, Clifton, NJ.
Birdsall NJM, Lazareno S, and Matsui H (1996) Allosteric regulation of muscarinic receptors. *Prog Brain Res* **109:**147–151.
Caulfield MP (1993) Muscarinic receptors: characterization, coupling and function. *Pharmacol Ther* **58:**319–379.
Colquhoun D (1971) *Lectures on Biostatistics*. Clarendon Press, Oxford, UK.
Ebihara S and Akaike N (1992) Strychnine-induced potassium current in CA1 pyramidal neurones of the rat hippocampus. *Br J Pharmacol* **106:**823–827.
Ehlert FJ, Roeske WR, Gee KW, and Yamamura HI (1983) An allosteric model for benzodiazepine receptor function. *Biochem Pharmacol* **32:**2375–2383.
Ehlert FJ, Roeske WR, and Yamamura HI (1994) Muscarinic receptors and novel strategies for the treatment of age-related brain disorders. *Life Sci* **55:**2135–2145.
Ellis J and Seidenberg M (1992) Two allosteric modulators interact at a common site on cardiac muscarinic receptors. *Mol Pharmacol* **42:**638–641.
Farrington H, Mendelsohn F, Chan S, Reinlib L, and Guggino SE (1994) Strychnine-binding proteins in intestinal cells: novel brucine binding site with binding affinities for alkaloids. *J Pharmacol Exp Ther* **271:**1074–1079.
Gnagey A and Ellis J (1996) Allosteric regulation of the binding of [^{3}H]acetylcholine to m2 muscarinic receptors. *Biochem Pharmacol* **52:**1767–1775.
Hejnova L, Tucek S, and El-Fakahany EE (1995) Positive and negative allosteric interactions on muscarinic receptors. *Eur J Pharmacol* **291:**427–430.
Hoare SR and Strange PG (1996) Regulation of D_2 dopamine receptors by amiloride and amiloride analogs. *Mol Pharmacol* **50:**1295–1308.
Hollmann M and Heinemann S (1994) Cloned glutamate receptors. *Annu Rev Neurosci* **17:**31–108.
Hulme EC, Birdsall NJM, and Buckley NJ (1990) Muscarinic receptor subtypes. *Annu Rev Pharmacol Toxicol* **30:**633–673.
Jakubik J, Bacakova L, El-Fakahany EE, and Tucek S (1997) Positive cooperativity of acetylcholine and other agonists with allosteric ligands on muscarinic acetylcholine receptors. *Mol Pharmacol* **52:**172–179.
Jakubik J, Bacakova L, Lisa V, El-Fakahany EE, and Tucek S (1996) Activation of muscarinic acetylcholine receptors via their allosteric binding sites. *Proc Natl Acad Sci USA* **93:**8705–8709.
Kollias-Baker C, Ruble J, Dennis D, Bruns RF, Linden J, and Belardinelli L (1994) Allosteric enhancer PD 81,723 acts by novel mechanism to potentiate cardiac actions of adenosine. *Circ Res* **75:**961–971.
Lazareno S and Birdsall NJM (1993) Estimation of competitive antagonist affinity from functional inhibition curves using the Gaddum, Schild and Cheng-Prusoff equations. *Br J Pharmacol* **109:**1110–1119.
Lazareno S and Birdsall NJM (1995) Detection, quantitation, and verification of allosteric interactions of agents with labeled and unlabeled ligands at G protein-coupled receptors: interactions of strychnine and acetylcholine at muscarinic receptors. *Mol Pharmacol* **48:**362–378.
Lefkowitz RJ, Cotecchia S, Samama P, and Costa T (1993) Constitutive activity of receptors coupled to guanine nucleotide regulatory proteins. *Trends Pharmacol Sci* **14:**303–307.
Macdonald RL and Olsen RW (1994) $GABA_A$ receptor channels. *Annu Rev Neurosci* **17:**569–602.
Mackerer CR, Kochman RL, Shen TF, and Hershenson FM (1977) The binding of strychnine and strychnine analogs to synaptic membranes of rat brainstem and spinal cord. *J Pharmacol Exp Ther* **201:**326–331.
Marvizon JCG, Vazquez J, Garcia Calvo M, Mayor FJ, Gomez AR, Valdivieso F, and Benavides J (1986) The glycine receptor: pharmacological studies and mathematical modeling of the allosteric interaction between the glycine- and strychnine-binding sites. *Mol Pharmacol* **30:**590–597.
Mascia MP, Machu TK, and Harris RA (1996) Enhancement of homomeric glycine receptor function by long-chain alcohols and anaesthetics. *Br J Pharmacol* **119:**1331–1336.
Massot O, Rousselle JC, Fillion MP, Grimaldi B, Cloez Tayarani I, Fugelli A, Prudhomme N, Seguin L, Rousseau B, Plantefol M, Hen R, and Fillion G (1996) 5-Hydroxytryptamine-moduline, a new endogenous cerebral peptide, controls the serotonergic activity via its specific interaction with 5-hydroxytryptamine$_{1B/1D}$ receptors. *Mol Pharmacol* **50:**752–762.
Matsui H, Lazareno S, and Birdsall NJM (1995) Probing of the location of the allosteric site on m1 muscarinic receptors by site-directed mutagenesis. *Mol Pharmacol* **47:**88–98.
Minton AP and Sokolovsky M (1990) A model for the interaction of muscarinic receptors, agonists, and two distinct effector substances. *Biochemistry* **29:**1586–1593.
Nunnari JM, Repaske MG, Brandon S, Cragoe EJ, and Limbird LE (1987) Regulation of porcine brain α_2-adrenergic receptors by Na^+, H^+ and inhibitors of Na^+/H^+ exchange. *J Biol Chem* **262:**12387–12392.
Pintor J, King BF, Miras-Portugal MT, and Burnstock G (1996) Selectivity and activity of adenine dinucleotides at recombinant $P2X_2$ and $P2Y_1$ purinoceptors. *Br J Pharmacol* **119:**1006–1012.
Proška J and Tuček S (1995) Competition between positive and negative allosteric effectors on muscarinic receptors. *Mol Pharmacol* **48:**696–702.
Schrattenholz A, Pereira EF, Roth U, Weber KH, Albuquerque EX, and Maelicke A (1996) Agonist responses of neuronal nicotinic acetylcholine receptors are potentiated by a novel class of allosterically acting ligands. *Mol Pharmacol* **49:**1–6.
Squires RF and Saederup E (1987) $GABA_A$ receptor blockers reverse the inhibitory effect of GABA on brain-specific (^{35}S)TBPS binding. *Brain Res* **414:**357–364.
Tränkle C and Mohr K (1997) Divergent modes of action among cationic allosteric modulators of muscarinic M_2 receptors. *Mol Pharmacol* **51:**674–682.
Tuček S, Musilkova J, Nedoma J, Proška J, Shelkovnikov S, and Vorlicek J (1990) Positive cooperativity in the binding of alcuronium and *N*-methylscopolamine to muscarinic acetylcholine receptors. *Mol Pharmacol* **38:**674–680.
Tuček S and Proška J (1995) Allosteric modulation of muscarinic acetylcholine receptors. *Trends Pharmacol Sci* **16:**205–212.
Waelbroeck M (1994) Identification of drugs competing with *d*-tubocurarine for an allosteric site on cardiac muscarinic receptors. *Mol Pharmacol* **46:**685–692.
Waelbroeck M, Robberecht P, de-Neef P, and Christophe J (1988) Effects of *d*-tubocurarine on rat cardiac muscarinic receptors: a comparison with gallamine. *J Recept Res* **8:**787–808.
Yeomans JS (1995) Role of tegmental cholinergic neurons in dopaminergic activation, antimuscarinic psychosis and schizophrenia. *Neuropsychopharmacology* **12:**3–16.

Send reprint requests to: Dr. S. Lazareno, MRC Collaborative Centre, 1–3 Burtonhole Lane, Mill Hill, London NW7 1AD, United Kingdom. E-mail: s-lazare@nimr.mrc.ac.uk

MOL PHARM

MOLECULAR PHARMACOLOGY

Erratum

In the article by Lazareno et al. [Lazareno S, Gharagozloo P, Kuonen D, Popham A and Birdsall NJM (1998) Subtype-selective positive cooperative interactions between brucine analogues and acetylcholine at muscarinic receptors: Radioligand binding studies. *Mol Pharmacol* **53:**573–589], there was an error in eq. 5. The corrected equation appears below. The authors regret any inconvenience caused by this error.

$$B_{LAXt} = B_{LAX} + (B_{L_o} - B_{LAX}) \cdot \left(\exp\left(\frac{-t \cdot k_{off}}{1 + \alpha X.K_X} + \frac{-t \cdot k_{off} \cdot L.K_L}{1 + X.K_X + (A.K_A)^n \cdot (1 + \beta.X.K_X)} \right) \right)$$